Enhanced softwood cellulose accessibility by H_3PO_4 pretreatment: high sugar yield without compromising lignin integrity

Journal:	*Industrial & Engineering Chemistry Research*
Manuscript ID	Draft
Manuscript Type:	Article
Date Submitted by the Author:	n/a
Complete List of Authors:	Rahaman, Mohammad Shahinur; University of Louisville, Hossain, Md. Anwar; University of Louisville Lee, David; University of California Berkeley Phung, Thanh; University of Louisville Canlas, Christian; King Abdullah University of Science and Technology, Simmons, Blake; Lawrence Berkeley Laboratory Renneckar, Scott; University of British Columbia, Wood Sciences Department Reynolds, William; Virginia Polytechnic Institute and State University, Material Science & Engineering George, Anthe; Sandia National Laboratories California, Tulaphol, Sarttrawut; King Mongkut's University of Technology Thonburi Sathitsuksanoh, Noppadon; University of Louisville, chemical engineering

Enhanced softwood cellulose accessibility by H_3PO_4 pretreatment: high sugar yield without compromising lignin integrity

Mohammad Shahinur Rahaman[1ξ], Anwar Hossain[1ξ], David Lee[2], Thanh Khoa Phung[1], Christian G. Canlas[3,4], Blake A. Simmons[2,6], Scott Renneckar[7], William Reynolds[8], Anthe George[2,5]*, Sarttrawut Tulaphol[1,9,*], and Noppadon Sathitsuksanoh[1*]

[1] Department of Chemical Engineering, University of Louisville, Louisville, KY 40292, USA
[2] Joint BioEnergy Institute, 5885 Hollis St, Emeryville, CA 94608, USA
[3] King Abdullah University of Science and Technology (KAUST), Core Labs, Thuwal, 23955-6900 Saudi Arabia
[4] College of Chemistry, University of California, Berkeley, CA 94720, USA
[5] Sandia National Laboratories, 7011 East Ave, Livermore, CA 94551, USA
[6] Lawrence Berkeley National Laboratory, 1 Cyclotron Rd, Berkeley, CA 94720, USA
[7] Faculty of Forestry, University of British Columbia, Vancouver, Canada
[8] Department of Materials Science & Engineering, Virginia Tech, Blacksburg, VA 24061, USA
[9] Department of Chemistry, King Mongkut's University of Technology Thonburi, Bangkok, 10140, Thailand
[ξ] These authors contributed equally to this work
* Corresponding author: Email: ageorge@lbl.gov, sarttrawut.tul@kmutt.ac.th, n.sathitsuksanoh@louisville.edu

Abstract

Softwood lignocellulose is a potential feedstock for production of biofuels and bioproducts. However, the highly cross-linked nature of softwood lignocellulose restricts enzyme access to its sugars. Thus, harsh pretreatment conditions (180 – 280°C) and/or high enzyme loading are required to unlock sugars. These requirements negatively affect the economic viability of softwoods in biorefineries. Here we show that H_3PO_4 pretreatment of pine and Douglas fir under a mild reaction temperature (50°C) and atmospheric pressure enabled a high (~80%) glucan digestibility with low enzyme loading (5 FPU/g glucan). The dissolution and regeneration of softwoods disrupted the hydrogen bonding between cellulose chains, thereby increasing the cellulose accessibility to cellulase (CAC) values by ~38-fold (from ~0.4 to 15 m^2/g biomass). Examination of H_3PO_4-pretreated softwoods by Cross Polarization/Magic Angle Spin (CP/MAS), ^{13}C- Nuclear Magnetic Resonance (NMR), and Fourier-transform Infrared Spectroscopy (FTIR) revealed that breaking of the orderly hydrogen bonding of crystalline cellulose caused the increase in CAC (higher than 11 m^2/g biomass), which, in turn was responsible for the high glucan digestibility of pretreated softwoods. The H_3PO_4 pretreatment process was feedstock independent. Lastly, 2D ^{13}C-^{1}H Heteronuclear Single Quantum Coherence (HSQC) NMR showed that the lignin was depolymerized but not condensed, thus, the lignin can be available for producing high-value products.

Keywords: Softwood, H_3PO_4, Lignocellulosic Biomass, Enzymatic hydrolysis

1. Introduction

Within 20 years, the number of automotive vehicles in use worldwide is projected to reach 2 billion [1] because of economic and population growth. Petroleum is the current feedstock for fuel production for these vehicles. Petroleum-derived fuels have two major drawbacks: (1) petroleum supply is limited, causing uncertainty in price and availability, and (2) processing petroleum generates carbon dioxide that contributes to global warming [2-3]. Clearly, an alternative fuel feedstock is urgently needed to supplement and/or replace petroleum.

Softwoods are woody biomass abundant in the northern hemisphere. Their high cellulose content, ~40-48% [4-6], makes them attractive renewable feedstocks for the production of biofuels and bioproducts [7]. The U.S. Department of Energy and the U.S. Department of Agriculture have estimated that ~1.4 billion tons of woody biomass and agricultural wastes will be available by the mid-21st century, providing vast feedstocks for biorefineries [8].

The guaiacyl (G)-type lignin monomer is the main lignin monomer in softwoods [9]. The G-type lignin monomer has a C_4 atom available to form a bond with other G-type lignin monomer units, creating highly cross-linked lignin. The cross-linked lignin is a strong glue that seals the cellulose from enzymes and catalysts during upgrading [4, 10-15]. Thus, typically, some type of pretreatment is required to provide cellulose accessibility to enzymes [16-17] to unlock sugars from lignocellulosic biomass [18]. For softwoods, severe pretreatment (e.g., 180-280°C) conditions are needed to expose cellulose to enzymes. These conditions present three challenges: (1) sugar degradation, (2) a requirement for high enzyme loadings due to generation of inhibitors (furfural, 5-hydroxymethylfurfural (HMF), and acetic acid) [12, 27, 16-17, 19-21], and (3) difficulty in further lignin utilization due to lignin condensation [22-23]. Solving these challenges is important for the economics of softwood biorefineries.

Cellulose solvents, including H_3PO_4 and various types of ionic liquids, are effective at lignocellulose dissolution/pretreatment. The dissolution of lignocellulose unglues the lignocellulose components by disrupting the lignin-carbohydrate complex (LCC) linkages, and it de-crystallizes the highly ordered cellulose structure by disrupting the intra/intermolecular hydrogen bonds between cellulose chains. De-crystallization of cellulose enhances its accessibility to acid/enzymes, enabling high glucan digestibility and fast hydrolysis rates with low enzyme loading [24-25]. In particular, pretreatment with the cellulose solvent H_3PO_4 (85%) breaks inter/intramolecular hydrogen bonds within lignocellulose and between cellulose chains under a mild condition (< 60°C and atmospheric pressure) [26-27]. Thus, H_3PO_4 pretreatment has been explored recently for agricultural wastes, bioenergy crops, and hardwoods [28-32]. The pretreated lignocellulose samples had high glucan digestibilities of > 73% with a low enzyme loading of 5 filter paper units (FPU) of enzyme/g glucan [33-35]. Various strategies have been developed to recycle these cellulose solvents [36-37]. Although H_3PO_4 pretreatment is effective at pretreating lignocellulose, its impact on softwoods and residual lignin after has not been assessed adequately.

In this contribution, we describe H_3PO_4 (85%) pretreatment at 50°C and atmospheric pressure for < 2h on southern yellow pine and Douglas fir, followed by enzymatic hydrolysis. Pretreated pine and Douglas fir had high glucan digestibility of ~80% with a low cellulase loading (5 FPUs/g glucan). We used a fusion protein to mimic and quantitate adsorption of cellulase enzymes onto the lignocellulose, Cross Polarization/Magic Angle Spin (CP/MAS) ^{13}C-Nuclear Magnetic Resonance (NMR) and Fourier-transform infrared (FTIR) spectroscopy to characterize changes in the degree of crystallinity, and 2D ^{13}C-^{1}H heteronuclear single quantum coherence (HSQC) NMR spectroscopy to elucidate changes in chemical structure of lignin after H_3PO_4 pretreatment. H_3PO_4 pretreatment enhanced cellulose accessibility to cellulase. The process disrupted LCC linkages and the highly ordered hydrogen bonds of cellulose, thereby reducing the degree of crystallinity. The pretreated materials became more amorphous compared with the untreated biomass. Moreover, this process did not modify lignin, enabling its potential profitable use in biorefineries.

2. Materials and Methods

2.1. Chemicals and materials

All chemicals were reagent grade and purchased from Sigma Aldrich (St. Louis, MO, USA), unless otherwise noted. Phosphoric acid (85% w/w) and ethanol (95% v/v) were purchased from Fisher Scientific (Houston, TX, USA). Microcrystalline cellulose, Avicel® PH105 (20 lm), was obtained from FMC Corp (Philadelphia, PA, USA). Regenerated amorphous cellulose (RAC) was prepared as described [38-39]. In short, (1) Avicel was mixed with water to make a slurry; (2) ice-cold 85% H_3PO_4 (~4°C) was added to the Avicel slurry and kept on ice for 1 h, and (3) deionized water was added to regenerate the RAC [40]. Trichoderma reesei cellulase (Novozyme® 50013) and β-glucosidase (Novozyme® 50010) were gifted by Novozymes North America (Franklinton, NC, USA). They had activities of 84 filter paper units (FPUs) of cellulase per mL and 270 units of β-glucosidase per mL. Southern yellow pine woodchips and Douglas fir were obtained from Brook Center at Virginia Tech (Blacksburg, VA, USA) and University of British Columbia (Vancouver, Canada), respectively. All naturally dried biomass samples were knife-milled by a Pallmann counter-rotating knife ring flaker (Clifton, NJ, USA). The resulting particulates with nominal sizes of 40–60 mesh (250–400 μm) were collected and used for all experiments.

*2.*2. H_3PO_4 pretreatment of softwoods

Pine and Douglas fir were pretreated with 85% H_3PO_4 as described [40-41]. In short, approximately 1.05 g of natural-dried biomass (~5% moisture) was mixed with 8 mL of 85% (w/w) H_3PO_4 in a 50 mL plastic centrifuge tube and heated at 50°C at atmospheric pressure for 105 min, unless otherwise noted. The pretreatment reaction was stopped by adding 20 mL of 95% (v/v) ethanol. Pretreated solid was separated by a swing bucket centrifuge at 4500 rpm for 10 min. The supernatant was removed. The pretreated solid was washed and centrifuged in a sequence of 40 mL of 95% (v/v) ethanol and 40 mL of deionized water two times, respectively. The resulting solid was neutralized with a 2 M sodium carbonate solution and stored in the presence of 0.1% (w/v) NaN_3 at 4°C to prevent microbial growth prior to enzymatic hydrolysis.

2.3. Enzymatic hydrolysis

The pretreated softwood was suspended to obtain 10 g glucan per liter in a 50 mM sodium citrate buffer (pH ~4.8) supplemented with 0.1% (w/v) NaN_3 (to prevent microbial growth) in a 50 mL centrifuge tube. Enzyme loadings were the following: (1) 5 FPUs of cellulase and 10 units of β-glucosidase per gram of glucan; or (2) 15 FPUs of cellulase and 30 units of β-glucosidase per gram of glucan, unless otherwise noted. The cocktail (pretreated samples + buffer solution + enzyme) was suspended in an incubator shaker at 50^{o}C and 600 rpm; samples were collected for 72 h. The cocktail samples were centrifuged at 13,000 rpm for 5 min to separate clear solution from the suspended solid. Exactly 500 μL of the supernatant was transferred to a 2 mL microcentrifuge tube maintained at room temperature for 30 min to allow cellobiose to be continuously converted to glucose by the residual enzyme. This step was important to ensure accurate enzymatic hydrolysis results. The supernatant was then acidified by adding 30 μL of 10% (w/w) sulfuric acid, followed by freezing overnight. The frozen sample was thawed, mixed well, and centrifuged at 13,000 rpm for 5 min to remove any precipitated solids. The supernatant, containing soluble sugars after enzymatic hydrolysis, was processed with an 1110 Agilent High-Pressure Liquid Chromatography system (HPLC, Agilent Technologies, Santa Clara, CA, USA). Enzymatic glucan digestibility was calculated as follows:

$$\text{Glucan digestibility (\%)} = \frac{\text{Glucan}_{\text{supernatant}}}{\text{Glucan}_{\text{pretreated biomass}}} \text{x100}$$

After 72 h enzymatic hydrolysis, the residual solid was washed with 20 mL deionized water to remove soluble sugars and enzyme prior to freeze-drying overnight. All experiments were conducted in triplicate and the standard deviations were calculated. The composition of the residual solid was then analyzed to construct the mass balance. X /0pp

2.4. Compositional analysis of softwoods and glucose determination

Compositional analysis of softwoods and residual enzymatic hydrolysis solids was performed by the NREL LAP procedure [42-43]. Briefly, 0.2 g of the sample was dissolved in 2 ml of 72 % H_2SO_4 at 30°C for 1 h in an incubator shaker prior to dilution of the H_2SO_4 concentration to 4% with deionized water. The sample was autoclaved at 121°C, 15 psi for 1 h and then filtered by a ceramic filter crucible. The filtrate was analyzed by HPLC for soluble sugars. Residual solids were dried at 105°C overnight. The weight of the dried solids corresponded to the amount of lignin and ash in the sample. The weight loss of the dried sample and residual weight after calcination at 575°C for 8 h corresponded to the amount of lignin and ash, respectively, in the sample.

Soluble sugars were measured by HPLC equipped with a refractive index detector (RID) and diode array detector (DAD). A Bio-Rad Aminex HPX-87P column (Richmond, CA, USA) was used to analyze soluble sugars with a rate of 0.6 mL/min of 4 mM H_2SO_4 as a mobile phase at 60°C. All sugars were calibrated against certified standards (Absolute Standards Inc., Hamden, CT, USA).

2.7. Characterization of softwoods before and after H_3PO_4 pretreatment

The Total Substrate Accessibility to Cellulase (TSAC), Cellulose Accessibility to Cellulase (CAC), and Non-Cellulose Accessibility to Cellulase (NCAC) were determined based on the maximum adsorption of the TGC fusion protein. This fusion protein contained thioredoxin (T), Green Fluorescent Protein (GFP), and three cellulose-binding modules (C). Fusion protein was used in the presence and absence of Bovine Serum Albumin (BSA) [40, 44]. TSAC was calculated by the maximum adsorption of TGC in the absence of BSA, whereas CAC was calculated by the maximum adsorption of TGC in the presence of BSA. NCAC was calculated by the difference between TSAC and CAC. TGC fusion protein was produced in Escherichia coli BL21 (pNT02), purified by adsorption onto regenerated amorphous cellulose (RAC), and desorbed with ethylene glycol (EG) [45]. EG was removed by dialysis in a 50 mM sodium citrate buffer (pH 6.0) and the TGC solution was concentrated using Millipore 10 kDa molecular weight cut-off centrifugal ultrafilter columns (Spectrum Lab, Billerica, MA, USA). Confocal microscopy was performed to confirm the presence of TGC on biomass. The confocal images were recorded on the Zeiss Axio Observer Z1 inverted microscope for fluorescence or brightfield microscopy (Carl Zeiss Microscopy, LLC, Thornwood, NY, USA)

Scanning Electron Microscopy (SEM). SEM images of the biomass materials were taken with a Zeiss-DSM940 (Carl Zeiss, Okerkochen, Germany), as described [35]. All samples were sputter-coated with gold prior to SEM imaging.

Attenuated Total Reflection (ATR) Fourier-transform infrared (FTIR) Spectroscopy. ATR-FTIR was conducted using a Thermo Nicolet 6700 ATR/FT-IR spectrometer (Thermo Fisher Scientific Inc., Waltham, MA, USA). Two hundred and fifty-six scans at a resolution of 6 cm^{-1} were averaged for each sample. The samples were scanned in the spectral range between 400 and 4000 cm^{-1}. The absorbances of the bands were resolved using Voigt distribution function by PeakFit1 4.12 software (Systat Software Inc., Chicago, IL, USA).

Cross Polarization/Magic Angle Spin (CP/MAS) ^{13}C-Nuclear Magnetic Resonance (NMR). The CP/MAS ^{13}C-NMR spectra of all samples were acquired with a Bruker Avance I 500-MHz NMR spectrometer operating at the resonance frequencies of 500.23 MHz for ^{1}H and 125.80 MHz for ^{13}C, using a double-resonance Bruker 4.0-mm broad-band CP-MAS probe spinning at 13–14 kHz. Cross polarization for 2-ms contact time was achieved using a ^{1}H 90° pulse width of 4.2 μs at 60-kHz two-pulse phase-modulated proton decoupling field and 2-s recycle delay. Total accumulation time was between 1000 and 3000 transients. All spectra were collected at room temperature and referenced against the chemical shifts of adamantane at 38.48 and 29.45 ppm. According to the C_4 peak-deconvolution method [46], the degree of crystallinity was determined and expressed as crystallinity index (CrI). The CrI value was calculated from the ratio of the crystalline area over the total area, for which the separation of crystalline ($\delta_{86–92}$ ppm) and amorphous ($\delta_{79–86}$ ppm) fractions was based on Gaussian line shape function.

2D ^{13}C-^{1}H heteronuclear single quantum coherence (HSQC) NMR spectroscopy. Softwood samples were extracted to remove extractives and ball milled as described [47-48]. The ball-milled softwood sample was mixed in a microcentrifuge tube with DMSO-d_6 and a minute amount of 1-ethyl-3-methylimidazolium acetate as a co-solvent [49-50]. This solution was sonicated in a Branson 2510 table-top cleaner (Branson Ultrasonic Corporation, Danbury, CT, USA) until it became a homogenous gel. The temperature of the sonication bath was maintained below 55°C. The homogeneous gel was transferred to the NMR tube. HSQC spectra were acquired at 25°C using a Bruker Avance-600 MHz instrument equipped with a 5 mm inverse-gradient $^{1}H/^{13}C$ cryoprobe and the q_hsqcetgp pulse program (ns = 200, ds = 16, number of increments = 256, d_1 = 1.0 s) [51]. Chemical shifts were referenced to the central DMSO peak (δ_C/δ_H 39.5/2.5 ppm). Assignments of the HSQC spectra were described elsewhere [47, 52]. A semi-quantitative analysis of the volume integrals of the HSQC correlation peaks was performed using Bruker's Topspin 3.1 (Windows) processing software. A Gaussian apodization in F_2 (LB = -0.50, GB = 0.001) and squared cosine-bell in F_1 (LB = -0.10, GB = 0.001) were applied prior to 2D Fourier Transformation.

3. Results and Discussion

The pine and Douglas fir samples consisted of ~35-39 wt.% glucan, 9-12 wt.% mannan, 3-6 wt.% xylan, and 33-34 wt.% lignin **(Table S1)**. The high mannan content was a signature of softwoods. Our softwood compositions agreed with previously reported values [20, 53]. High lignin content in softwoods and its highly cross-linked G-type lignin structure are barriers for enzymes and/or catalysts to access cellulose. Our strategy to circumvent this barrier was to employ H_3PO_4 pretreatment to disrupt the lignin-carbohydrate complex (LCC) linkages and intra/intermolecular hydrogen bonds between crystalline cellulose chains of softwoods.

3.1. Effect of H_3PO_4 pretreatment of softwood on enzymatic hydrolysis

Untreated pine and fir showed a low glucan digestibility of < 7% after 72h with 15 FPUs/g glucan of enzyme loading. These results illustrated the high recalcitrance of softwoods. Conversely, pretreated pine and Douglas fir had a fast hydrolysis rate and their glucan digestibilities were > 72% after 12h, reaching a maximum of 87% after 72h for Douglas fir at 15 FPU/g glucan enzyme loading. A 3-fold reduction in enzyme loading (5 FPU/g glucan) still yielded a fast hydrolysis rate and high glucan digestibilities of >63% after 12h and >80% after 72h for both softwoods **(Fig. 1).** These results confirmed that H_3PO_4 pretreatment was efficient for softwoods, thus, we obtained a high glucan digestibility (>63%) after 12h at a low cellulase loading.

Pretreatment cost represents about 20% of the total cost in biomass conversion processes [54]. The harsh reaction conditions (high temperature: 170 - 200°C and 6.5 – 7.2 bar) and/or high enzyme loading add significantly to capital expenditure (CAPEX) and operating expenditure (OPEX) of the overall process. Moreover, a harsh reaction condition (high temperature >120^{o}C) possibly cleaves β-O-4 lignin linkage and forms undesired condensed C-C linkages [55], limiting lignin's potential upgrading to co-products.

The H_3PO_4 pretreatment showed a high glucan digestibility (78% for pine and 80% for Douglas fir) with a low enzyme loading (5 FPUs/g glucan) at mild condition (50°C under atmospheric pressure). H_3PO_4-pretreated softwoods were rapidly enzymatically hydrolyzed with the release of a high amount of glucose. Moreover, our results suggested that we could reduce the cellulase enzyme loading by 3-fold (5 FPUs/g glucan) and still maintain a high glucan digestibility (>78%) of pretreated pine and Douglas fir.

Previous studies on softwoods performed with the aforesaid harsh pretreatment conditions (**Table1**) did demonstrate high sugar yield [19, 56-58]. For example, Shuai et al. studied spruce pretreatment by Sulfite Pretreatment to Overcome Recalcitrance of Ligno-cellulose (SPORL) and by Dilute Acid (DA) pretreatment at 180°C for 30 min and obtained 91% and 55 % glucan digestibility, respectively, with 15 FPUs/g glucan enzyme loading [19]. A decrease in enzyme loading from 10 to 5 FPUs/g glucan dropped the glucan digestibility of SPORL-pretreated spruce from 91% to 70% [19]. Nonetheless, this and similar approaches do not mitigate the high economic cost of conversion.

The green chemistry environmental factor (E-factor) metric has become an important indicator of the sustainability of a process (see *Supplementary Information*) [59-60]. To the best our knowledge, we are the first to use E-factor to describe pretreatment processes. The E-factor values ranged from 1.1 to 80.3 (**Table 1**). Ball milling, steam explosion, wet explosion, and SO_2-steam explosion had the lowest E-factors (1.1-1.8). One reason for the low E-factors is that these pretreatments do not use chemicals. However, they do use a high enzyme loading of 114 FPU/g glucan (173 mg protein/g glucan) to achieve the moderate glucan digestibility of 63% from ball-milled pretreated softwoods. Although the combined physical and chemical pretreatments result in high glucan digestibility (70-96%), the tradeoff is that they use a harsh pretreatment conditions as reflected in a high severity factor (log R_0) of 3.54-5.0. For example, the combined SO_2-steam explosion + alkali-based pretreatments yield a glucan digestibility of 90-94% after 48h with a high severity factor (log R_0) [61] of ~4-5 (see *Supplementary Information*).

Our H_3PO_4 pretreatment process showed a moderate E-factor of 49.7. However, our approach had several advantages. First, the H_3PO_4 pretreated softwoods had a high glucan digestibility of ~78-80% with a low enzyme loading (5 FPUs/ g glucan) and a high reaction rate. The enzyme cost in biofuels production is ~$0.68/gal (based on theoretical sugar yields from lignocellulosic biomass) or $1.47/gal (based on saccharification and fermentation yields) of bioethanol [62-63]. Hence, reduction of enzyme loading while maximizing sugar yield is important for economic feasibility. Second, the H_3PO_4 pretreatment was conducted at a mild reaction condition of 50°C under atmospheric pressure as shown in the low severity factor of 0.91. To achieve high glucan digestibility of softwoods, a severity factor of > 3 is a commonplace (**Table S3**). We found a linear correlation between severity factor (log R_o) and glucan digestibility (**Fig. S2**). Although this correlation suggested that a high glucan digestibility can be achieved at severe pretreatment condition, the high severity factor (see *Supplementary Information*) translates to high energy consumption, contributing to the production cost. The H_3PO_4 pretreatment under a mild reaction condition (low temperature and no pressure) can reduce the energy in the biorefinery process.

However, H_3PO_4 recycling should also be considered to make this process economical. Several recycling processes, such as liquid extraction [64-65] and diffusion dialysis [66], show potential in recycling H_3PO_4 with high purity (80-90% acid recovery). Moreover, spent H_3PO_4 can be used to produce fertilizer [67]. The development of the techno-economic analysis (LCA) model and life cycle analysis (LCA) of this process are underway. In sum, the H_3PO_4 pretreatment process reduces energy consumption, reduces enzyme loading, and likely, will reduce the operating cost for biorefineries. These reasons make H_3PO_4 pretreatment an attractive approach for practical applications.

Table 1. Pretreatment technologies for softwoods

	Pretreatment	Feedstock	Pretreatment Condition	Enzyme loading (FPU/g glucan)[a]	Protein conc. (mg protein/g glucan)[b]	Glucan digestibility	E-factor[c]	Severity (log R_o)	Ref
Cellulose solvent	H_3PO_4 pretreatment	Yellow pine	50°C, 1.45-2 h	5	10	78% @ 48h	49.7	0.91	This study
		Douglas fir		15	30	80% @ 48h			
	Cholinium lysinate ([Ch][Lys])	Pine	140°C, 1 h	14.8	20	23% @ 72h	80.3	2.96	68
	1-butyl-3-methylimidazolium chloride ([Bmim]Cl)	Pine (Pinus rigida & Pinus densiflora)	130°C, 18 h	17.5	37	97% @ 96 h	79.8	3.92	69
	N,N-dimethylbutylammonium hydrogen sulfate ([DMBA][HSO_4])	Pine	170°C, 30 min	16.4	20	75% @ 168h	22.7	3.54	70
Physical	Ball-milling	Douglas fir	10-min milling and 10-min pausing for 240 min	114	173	~ 63% @ 72 h	1.7	0.17	56
Chemical	Dilute acid	Spruce	180°C, 30 min	15	84	59.5% @ 48 h	26.4	3.83	19
	Ethanol organosolv	Douglas fir	188°C, 15 min	14	35	> 90% @ 24h	22.0	3.77	71
	Ethanol organosolv	Loblolly pine	170°C, 1h	8	32	61% @ 80h	27.9	3.84	58
Physico-chemical	Wet explosion	Loblolly pine	170ºC, 7.2 bar O_2, 22 min	44	66	96% @ 72 h	1.8	3.54	57
	Sulfite pretreatment	Spruce	180°C, 30 min	15	84	91% @ 24 h	21.9	3.83	19
				5	28	70% @ 48 h			
	Steam pretreatment	Douglas fir	160°C, 10 min	n.d.	n.d.	~ 80% @ 72 h	1.7	2.77	72
	SO_2-steam explosion	Lodgepole pine	215°C, 5 min	20	114	94% @ 48h	1.3	4.08	73
	SO_2-steam explosion	Douglas fir	210°C, 5 min	60	218	> 95% @72h	1.1	3.94	74
	SO_2-steam explosion + alkaline peroxide treatment	Douglas fir	195°C, 4.5 min + 80°C, 45 min	10	37	90% @ 48h	56.7	4.49[d]	75
	SO_2-steam explosion + alkaline peroxide treatment	Douglas fir	195°C, 4.5 min + 80°C, 45 min	20	50	> 95% @ 48h	27.9	4.49[d]	71
	SO_2-steam explosion + alkali-oxygen treatment	Douglas fir	195°C, 4.5 min + 110°C, 3h	20	79	81% @48h	44.0	5.06[d]	76
				40	158	90% @48h	39.5		

[a] *Enzyme loading was calculated under the assumption as summarized in* ***Table S2****.*

[b] *Protein concentration (including cellulase and β-glucosidase enzymes) was calculated by the weight of total protein loaded per weight of glucan (Table S2).*

[c] *E-factor was calculated only from the mass balance information of pretreatment, excluding waste from washing steps after pretreatment (Table S3).*

[d] *Severity factor was calculated based on the severest condition (Table S3).*

n.d. = No data

3.2. Mass balance of the pretreatment and enzymatic hydrolysis of pine and Douglas fir

To understand the economics of the process, we constructed the mass balance on the basis of 100 g of softwood **(Fig. 2)**. The solid recovery was 78% and 81% for pretreated pine and Douglas fir. We obtained a high glucan recovery, ~90%, from pretreated pine and Douglas fir, whereas xylan recovery was low (~10%) **(stream 3)**. These results suggested that ethanol could efficiently recover most dissolved glucan and simultaneously fractionate xylan in the liquid stream. We observed a slight decrease (~15%) in lignin content after H_3PO_4 pretreatment **(stream 3)**, suggesting that most lignin remained in the solid. After enzymatic hydrolysis, we achieved 80% glucan digestibility for pretreated pine (28.0 g glucose/100g dry weight) and 79% (31.2 g glucose/100g dry weight) for pretreated Douglas fir **(stream 5)**. The overall glucose yields were 82% for pine and 80% for Douglas fir (**streams 2 + 5**). Moreover, the overall xylose yield was ~90% for both pretreated softwoods.

The main barriers to softwood conversion are (1) inter/intramolecular hydrogen bonding networks within cellulose chains that form highly ordered crystalline cellulose; and (2) lignin-carbohydrate complex (LCC) linkages [40, 77]. To design and optimize the process for other types of softwood lignocellulose, we need to more completely understand the factors that contribute to high glucan digestibility. Accordingly, as described next, we characterized the morphology and accessibility of cellulose, the cellulose surface functionalities, changes in cellulose crystallinity, and changes in the chemical structure of lignin of pretreated softwoods.

3.3. Fusion protein assessment of morphology and cellulose accessibility of pretreated softwoods

Pretreatment of softwoods disrupted their fibrous structure. **(Fig. 3).** SEM Figures 3A & B show the clear fibrous structures of untreated pine and Douglas fir, and Figures 3C & D show disrupted structures after H_3PO_4 pretreatment. Disruption of fibrous structure may have been due to swelling of the cellulose induced by phosphate ions adding to hydroxyl groups. Phosphate addition would form cellulose phosphate bridges (cellulose-O-PO_3H_2) [78-80]. These bridges stretch cellulose chains away from each other in the crystalline cellulose, resulting in swelling and disruption of the fibrous structure. Addition of anti-solvent (ethanol or water) converted cellulose phosphate to free phosphate and amorphous cellulose [79-80], which was more susceptible to enzymatic hydrolysis.

The formation of amorphous cellulose also suggested an enhanced surface accessibility. A common method to determine the surface accessibility of materials is the N_2 adsorption-desorption technique [81-82]. For our purpose, the drawback of this technique is that the N_2 molecule is small compared with the cellulase enzyme. Hence, N_2 adsorption/desorption may over-estimate the surface accessibility to enzymes. A more accurate quantitative assay to determine cellulose accessibility to enzymes is based on adsorption of a non-hydrolytic fusion protein (TGC) to the cellulose surface [83-84]. The TGC protein is 62 kDa, similar in size to *Trichoderma reesei endo*-glucanase I [85-86]. Moreover, TGC had the cellulose-binding module (CBM) to mimic cellulase adsorption onto cellulose. The green fluorescent protein (GFP) moiety in TGC reports the adsorbed area under fluorescence microscopy (**Fig. S1A**). TGC non-specifically adsorbs onto lignocellulosic biomass (cellulose, hemicellulose, and lignin) (**Fig. S1B**). Thus, we first blocked non-specific TGC adsorption by incubating untreated and pretreated softwoods with bovine serum albumin (BSA), which was allowed to bind onto the non-cellulosic portions of the softwoods. Then TGC could bind to the cellulosic portion (**Fig. S1C**). TGC adsorption followed a Langmuir adsorption isotherm and enabled the calculation of cellulose accessibility to cellulase (CAC) [84]. TGC adsorption onto the untreated and pretreated softwoods without BSA blocking enabled calculation of the total substrate accessibility to cellulase (TSAC). Hence, the non-cellulose accessibility to cellulase (NSAC) is calculated from the difference between TSAC and CAC.

Untreated Douglas fir had a low TSAC value of ~0.58 m^2/ g biomass and untreated pine had a similarly low value of 0.75 m^2/ g biomass **(Fig. 4)**. The CAC value was 0.40 m^2/ g biomass for Douglas fir and 0.43 m^2/ g biomass for pine. Because TSAC measurement accounted for the non-cellulose accessibility to cellulase (NSAC), the TSAC value of untreated and pretreated softwoods was higher than CAC. After pretreatment, TSAC values increased 27-fold (from 0.6 to 16 m^2/ g biomass) for Douglas fir and 20-fold (0.8 m^2/ g biomass to ~16 m^2/ g biomass) for pine **(Fig. 4)**. Similarly, CAC values increased after pretreatment, ~38-fold (from ~0.4 to 15 m^2/ g biomass) for both Douglas fir and pine. This 38-fold increase in CAC value explains the high susceptibility of pretreated pine and Douglas fir (> 80% glucan digestibility) to enzymatic hydrolysis at a low digestibility under 15 FPUs cellulase/g glucan). These increases in TSAC and CAC also explained the disappearance of the fibrous structure observed in the SEM micrographs after pretreatment.

A high CAC value is important to achieve high glucan digestibility. Typically, untreated biomass has a low CAC value due to the crystalline nature of cellulose, hemicellulose, and lignin [38, 87-88]. After pretreatment, the CAC value increases because of improvement in the accessible surface area from breaking the highly ordered hydrogen bonding of crystalline celluloses and/or removal of hemicellulose/lignin. Thus, the mode of pretreatment is important. Lignin glues plant components together. It was commonly believed that lignin removal would increase the surface accessibility of enzymes to cellulose substrate. Rollin et al. compared two pretreatment techniques that either targeted lignin removal or increased cellulose accessibility [38, 87-88]. They found that increasing cellulose accessibility was more important than lignin removal to achieve a high glucan digestibility. We also found a correlation between CAC and glucan digestibility (**Fig. S3**). An increase in CAC >11 m^2/g biomass from H_3PO_4 pretreatment improved glucan digestibility to >80%.

3.4. Changes in surface functionalities of softwoods after H_3PO_4 pretreatment

Pretreatment with H_3PO_4 improved cellulose accessibility by converting crystalline cellulose to amorphous cellulose and unwrapping hemicellulose and lignin from the cellulose. This finding was established by FTIR investigation of changes in surface chemical functionality. Normalized FTIR spectra of pine and Douglas fir showed similar bands at 808 (in-phase ring glucomannan), 895 (anomeric vibration at β-glycosidic linkage), 1263 (C-O stretching in guaiacyl ring), 1430 (CH_2 bending vibration from cellulose and lignin), 1451 (C-H deformations of lignin), 1507 (aromatic ring stretch in lignin), 1595 (aromatic skeletal vibrations and C=O stretch), and 1730 (ketone/aldehyde C=O stretching) **(Fig. 5, Table S4)** [89-93]. Galactoglucomannan is the principal hemicellulose in softwoods [94]. The hydroxyl groups at the C_2- and C_3-positions in the backbone units are partly substituted by *O*-acetyl groups, giving rise to the acetyl group band at 1730 cm^{-1} [95]. The vibration mode related to the acetyl groups at 1730 cm^{-1} [96] disappeared after pretreatment, suggesting deacetylation. The disappearance of the acetyl groups corroborated the 70% hemicellulose removal in the mass balance during pretreatment (**Fig. 2**). The intensity of in-phase ring glucomannan peak at 808 cm^{-1} was reduced after pretreatment, confirming the removal of hemicelluloses [97]. Other absorbance regions related to lignin, including [58] in-plane C-H stretch at 1451 cm^{-1} [90] and C-O ring stretches at 1263 cm^{-1}, were greatly reduced after H_3PO_4 pretreatment [90, 98].

The band at 1430 cm^{-1} showed dominant cellulose I region. Cellulose I is the native form of cellulose in plants [99-100]. The band at 895 cm^{-1} showed dominant cellulose II and amorphous cellulose regions. After H_3PO_4 pretreatment, the pretreated softwoods showed an intensity reduction of the 1430 cm^{-1} peak and an increase in the intensity of the 895 cm^{-1} peak, indicating that H_3PO_4 had disrupted the highly ordered hydrogen bonding in cellulose and converted cellulose I to amorphous cellulose and/or cellulose II. Amorphous cellulose and cellulose II accelerated the overall rate of enzymatic hydrolysis because they are more accessible to enzymes compared with cellulose I [100].

These findings coincided with the disappearance of the fibrous structure shown by SEM and an increase in the CAC values after pretreatment. Moreover, hemicellulose and lignin, glued around the cellulose structure, were unwrapped after H_3PO_4 pretreatment, corresponding with the reduction of spectral intensities in acetal groups and lignin-carbohydrate linkages. In sum, H_3PO_4 pretreatment converted crystalline cellulose to amorphous cellulose by removing hemicellulose and lignin, and improving cellulose accessibility.

3.5. Changes in degree of crystallinity of softwoods after H_3PO_4 pretreatment

Intra/intermolecular hydrogen bonding within cellulose chains affects its chemical structure and the strength to hold the structure together. Cellulose crystallinity has an important effect on enzymatic hydrolysis. High crystallinity equals low cellulose accessibility by cellulase. Thus, we used CP/MAS ^{13}C NMR to determine the crystallinity index (CrI) of untreated and pretreated softwoods. Typically, changes in the C_4 region of cellulose informed us of the CrI of cellulose **(Fig. S4, blue region, adapted from [101])**. Changes in C_6 region suggested the breaking of hydrogen bonding between cellulose chains **(Fig. S4, orange region)** [102-103]. To establish the baseline, we first used Avicel® (crystalline cellulose) and RAC (amorphous cellulose) as controls. The Avicel spectrum had doublets at C_4 and C_6 regions. At the C_4 region of Avicel, the peak ~88.90 ppm indicated crystalline cellulose, whereas the peak at ~84.20 ppm indicated amorphous cellulose **(Fig. S5)** **[104]** The C_6 region peak at 65.35 ppm indicated strong hydrogen bonding between cellulose chains. We also observed a small shoulder peak ~62.80 ppm, indicating disordered hydrogen bonding between cellulose chains [104]. The CrIs of Avicel, RAC, untreated, and H_3PO_4-treated softwoods are shown in **Fig. 7**. Avicel had 51% CrI, suggesting that Avicel contained both crystalline and amorphous cellulose. The RAC spectrum showed a broad peak at C_4 region, suggesting disruption of hydrogen bonding and an amorphous state (compared with Avicel) **(Fig. S5)**. The C_6 region of RAC showed a disappearance of the peak at 65.35 ppm, causing a peak at 62.80 ppm to become more pronounced. The disappearance of the peak at 65.35 ppm suggested the breaking of hydrogen bonding between cellulose chains and RAC becoming more amorphous. However, we could not determine the CrI of RAC because we didn't observe a crystalline cellulose peak after H_3PO_4 pretreatment [34, 105]. Comparing Avicel with RAC, we found the difference in the C_4 region agreed with the difference in the C_6 region, suggesting that dissolving Avicel in 85% H_3PO_4 disrupted inter/intramolecular hydrogen bonding within the cellulose structure.

Untreated pine and fir showed doublets at C_4 and C_6 regions **(Fig. 6)**, suggesting that their cellulosic portion contained both crystalline and amorphous fractions. After pretreatment, the crystalline cellulose peaks at 88.90 ppm and 65.35 ppm of both pine and Douglas fir disappeared, indicating that crystalline cellulose became amorphous. We observed ~18% and 16% decrease in CrI of pine and Douglas fir after H_3PO_4 pretreatment. The decrease in CrI of pretreated pine and Douglas fir coincided with FTIR results that crystalline cellulose became more amorphous after H_3PO_4 pretreatment. Moreover, untreated pine and fir showed a peak near ~56 ppm, assigned to methoxyl groups in lignin [58], and we observed this peak after pretreatment. These results suggested that H_3PO_4 pretreatment did not remove much of the lignin, in agreement with the mass balance calculation that indicated 9-15% lignin removal.

3.6. 2D ^{13}C-^{1}H HSQC NMR spectra of softwood samples before and after pretreatment

To understand changes in the chemical structure of softwood lignins, we used 2D ^{13}C-^{1}H HSQC NMR to characterize their aliphatic (lignin side chain units, **Fig. 8**), anomeric (**Fig. 9**), and aromatic regions pre- and post-treatment (**Fig. 10**). The peak assignments of aliphatic, anomeric, and aromatic regions are summarized in **Table S5** [106-107].

Anomeric region. The HSQC spectra in the anomeric region of pine and Douglas fir provided information about the configuration and glycosidic linkages between sugar monomeric units [48]. Signals in these spectra are associated with oligosaccharides from cellulose and hemicelluloses. We assigned the cellulose peaks based on previously reported values [108-109]. The internal cellulose unit, (1→4)-β-D-Glc*p*, (δ_C/δ_H = 102.5/4.5 ppm) is the most important cellulosic component of the plant cell wall. The α- and β-anomeric reducing-end correlations of cellulose were well separated from the internal cellulose unit. For example, the α-D-Glc*p*(R) was at 92.7/5.2 ppm and β-D-Glc*p*(R) was at 97.1/4.44 ppm. In general, we observed reducing end unit cross-peaks in the anomeric region after pretreatment, but the internal cellulose peak became weaker, suggesting cleavage of glycosidic linkages by pretreatment.

In general, the higher frequency of reducing end correlations in the anomeric region suggests depolymerization of carbohydrates. Hence, we could estimate the cellulose degree of polymerization (DP) by integrating the cross-peaks of reducing end units and internal anomeric cellulose [109-110]. Our calculated cellulose DP was ~9 for untreated pine and ~5 for untreated Douglas fir. These low DP values might have been due to over-estimation of reducing end units, and the actual cellulose DP could have been higher [109]. For this study, we sought to investigate the relative change of the cellulose DP. After pretreatment, the cellulose DP decreased by 62% for pine and by 36% for Douglas fir. These decreases in cellulose DP suggested cleavage of hydrogen bonding. These results also coincided with the pretreatment changes in C_4 and C_6 regions observed by CP/MAS ^{13}C-NMR (**Fig. 6**), suggesting that inter/intramolecular hydrogen bonding between cellulose chains was disrupted. The disruption of hydrogen bonding resulted in an increase in cellulase accessibility to cellulose (**Fig. 4**).

Hemicellulose is another component that we observed in the anomeric region. Softwood hemicellulose is present as galactoglucomannans [111]. These galactoglucomannans contain acetyl groups on the (1→4)-β-mannosyl units at C_2 (2-*O*-Ac-β-D-Man*p)* and C_3 (3-*O*-Ac-β-D-Man*p)* positions [47, 112]. Our untreated pine and Douglas fir samples showed the cross-peak of 2-*O*-Ac-Man*p* (M_2), but we did not observe 3-*O*-Ac-Man*p* (M_3) peak. The disappearance of the M_3 peak might have occurred because it overlapped with the β-aryl ether (A_α). The M_2 cross-peak became weaker after pretreatment, suggesting that hemicelluloses were removed. These results corroborated our mass balance (**Fig. 2**), which showed that we removed ~79% of the xylan from pine and 90% from Douglas fir. We also removed ~63% mannan from pine and 66% from Douglas fir.

Aliphatic region. Lignin linkages of untreated softwoods consisted mainly of β-aryl ether (β-O-4 **A**) with resinol (β-β **B**) and a trace amount of phenylcoumaran (β-5 **C**). Pretreatment weakened the β-O-4 cross-peak, suggesting that the ether bonds were cleaved and lignin fragments were released. Using semi-quantitative analysis, we integrated these cross-peaks to determine the relative abundance of these lignin linkages (per 100 aromatic units) (**Table 2**). These calculated values of softwood lignin interunit linkages agreed with previously reported values for softwoods [113-116]. Our calculated values of lignin's interunit linkages revealed that β-O-4 was the most abundant, followed by β-5 and β-β. The pretreated softwoods showed ~45% reduction in β-O-4 **A** and a slight increase in β-5 **B,** whereas β-β **C** remained unchanged.

The bond dissociation enthalpy (BDE) of these lignin interunit linkages are in the following order: $BDE_{\beta\text{-O-4}}$ (65 kcal/mol) < $BDE_{\beta\text{-}\beta}$ (117 kcal/mol) < $BDE_{\beta\text{-5}}$ (125 kcal/mol) [117]. These BDE values agree with our results, showing that the β-O-4 was easier to be cleaved compared with β-5 and β-β. After pretreatment, a significant decrease in relative abundance of β-O-4 and maintenance of the β-5 and β-β similar to those of untreated softwoods suggested that lignin depolymerization was the dominant reaction as evidenced by a great decrease in the β-O-4 **A** with minimal carbon-carbon linkage degradation reaction (breaking β-β **C**) and condensation reaction (formation of β-5 **B**) [118]. The residual lignin from this pretreatment was depolymerized with minimal formation of C-C bonds, an outcome that provides the opportunity to upgrade the resulting lignin into high-value products (aromatic chemicals, battery components, and carbon fibers)[119-120] and to make this process economically viable [121].

Aromatic region. Lignin has three aromatic units, syringyl (S) unit, guaiacyl (G) unit and *p*-hydroxyphenyl (H) unit. The aromatic region of untreated pine and Douglas fir showed that both contained only guaiacyl (G) units, which was a signature of softwoods [19]. Examination of the aromatic region (**Fig. 10**) demonstrated that pretreated softwoods did not show any change in the signals of major aromatic units compared to that of untreated softwoods. These results suggested that, although H_3PO_4 pretreatment could hydrolyze lignin's β-aryl ether linkages into small lignin fragments, the remaining lignin in pretreated samples was not modified and/or condensed.

Table 2. Change in structure characteristic of lignin before and after H_3PO_4-pretreatment of pine and Douglas fir

Sample\lignin interunit linkages	**Relative abundant (%)**		
	β-O-4 A	**β-5 B**	**β-β C**
Untreated pine	74 (48)	19 (12)	6 (4)
Pretreated pine	61 (26)	33 (14)	6 (3)
Untreated Douglas fir	73 (47)	18 (12)	9 (6)
Pretreated Douglas fir	56 (26)	35 (16)	9 (4)

Note: values in parenthesis indicate the relative amount of interunit linkages per 100 aromatic units.

We have applied our H_3PO_4 pretreatment process to a variety of lignocellulosic feedstocks at a mild reaction temperature (50°C) and atmospheric pressure, including agricultural waste, bioenergy crops, and woody biomass (hardwoods and softwoods). H_3PO_4 pretreatment improved cellulose accessibility to cellulase, resulting in a high glucan digestibility of ~80-100% with a low enzyme loading of 5 FPUs/g glucan (**Fig. 11, adapted from** [88]). This process was biomass species-independent. Its mild reaction condition, high sugar yield at a low enzyme loading, and preservation of lignin will have a great impact on the economic viability of biorefineries.

4. Conclusion

We examined the H_3PO_4 pretreatment of pine and Douglas fir at low temperature (50^{o}C) and atmospheric pressure. This process showed low severity factor (0.91) and a moderate E-factor (49.7) compared with other pretreatment processes. After 48h, we achieved a high glucan digestibility of 78% for pine and 80% for Douglas fir, even at a low enzyme loading of 5 FPUs/g glucan. H_3PO_4 pretreatment produced cellulose accessibility to cellulase (CAC) values higher than the 11 m^2/g threshold, yielding >78% glucan digestibility at a low enzyme loading (5 FPU/g glucan). Examination of pretreated softwoods by CP/MAS, ^{13}C-NMR, and FTIR revealed breaking of the orderly hydrogen bonding of crystalline cellulose, which was responsible for an enhanced CAC value. The process was feedstock-independent. NMR revealed that lignin was depolymerized without being condensed, providing the opportunity to upgrade the pretreated lignin to value-added chemicals. In summary, the mild reaction condition, high sugar yield at a low enzyme loading, and preservation of lignin of our H_3PO_4 pretreatment process will have a great impact in the economics of the biorefinery.

Acknowledgment

A part of this work was supported by the National Science Foundation under Cooperative Agreement No. 1355438. Materials characterization was performed in part at the Conn Center for Renewable Energy Research at the University of Louisville, which belongs to the National Science Foundation NNCI KY Manufacturing and Nano Integration Node, supported by ECCS-1542174. This work was part of the DOE Joint BioEnergy Institute (http://www.jbei.org) supported by the U.S. Department of Energy, Office of Science, Office of Biological and Environmental Research, through contract DE-AC02-05CH11231 between Lawrence Berkeley National Laboratory and the U. S. Department of Energy. The publisher, by accepting this article for publication, acknowledges that the United States Government retains a non-exclusive, paid-up, irrevocable, worldwide license to publish or reproduce the published form of this manuscript, and allow others to do so, for United States Government purposes. The Department of Energy will provide public access to these results of federally sponsored research in accordance with the DOE Public Access Plan (http://energy.gov/downloads/doe-public-access-plan). The authors would like to thank Dr. Howard Fried for his valuable comments and suggestions on the manuscript.

List of Figures and Tables

Figure S2. Correlation of severity and glucan digestibility in various softwood pretreatment methods

Figure S3. Comparison of cellulose accessibility to cellulase (CAC) and glucan digestibility in various pretreatment methods.

Figure S4. Crystalline and amorphous regions in CP/MAS ^{13}C NMR spectrum of microcrystalline cellulose. C_4 and C_6 regions are typically used for CrI determination and evaluation of changes in inter/intramolecular hydrogen bonding.

Figure S5. CP/MAS ^{13}C-NMR spectra of Avicel® and Regenerated amorphous cellulose (RAC)

Table 1. Pretreatment technologies for softwoods

Table 2. Change in structure characteristic of lignin before and after H_3PO_4-pretreatment of pine and Douglas fir

Table S1. Compositions of Douglas fir and yellow pine

Table S2. Assumption of enzyme activity in different enzymes.

Table S3. Severity and environmental factors in different pretreatment methods.

Table S4. Characteristic peaks of the functional groups of softwood by FTIR

Table S5. ^{13}C-^{1}H correlation peak assignments of aliphatic, anomeric, and aromatic regions observed in softwoods

References

1. Voelcker, J. 1.2 Billion Vehicles On World's Roads Now, 2 Billion By 2035: Report. https://www.greencarreports.com/news/1093560_1-2-billion-vehicles-on-worlds-roads-now-2-billion-by-2035-report (accessed 3 June 2019).
2. Cleveland, C. J.; Morris, C., Section 45 - Climate Change. In *Handbook of Energy*, Cleveland, C. J.; Morris, C., Eds. Elsevier: Boston, 2014; pp 805-820.
3. Rackley, S. A., 4 - Carbon capture from power generation. In *Carbon Capture and Storage (Second Edition)*, Rackley, S. A., Ed. Butterworth-Heinemann: Boston, 2017; pp 75-101.
4. Alvarez-Vasco, C.; Zhang, X., Alkaline hydrogen peroxide pretreatment of softwood: Hemicellulose degradation pathways. *Bioresource Technology* **2013,** *150*, 321-327.
5. Pielhop, T.; Amgarten, J.; von Rohr, P. R.; Studer, M. H., Steam explosion pretreatment of softwood: the effect of the explosive decompression on enzymatic digestibility. *Biotechnology for Biofuels* **2016,** *9* (1), 152.
6. Gschwend, F. J. V.; Chambon, C. L.; Biedka, M.; Brandt-Talbot, A.; Fennell, P. S.; Hallett, J. P., Quantitative glucose release from softwood after pretreatment with low-cost ionic liquids. *Green Chemistry* **2019,** *21* (3), 692-703.
7. Peleteiro, S.; Garrote, G.; Santos, V.; Parajó, J. C., Furan manufacture from softwood hemicelluloses by aqueous fractionation and further reaction in a catalyzed ionic liquid: a biorefinery approach. *Journal of Cleaner Production* **2014,** *76* (Supplement C), 200-203.
8. Perlack, R. D., *Biomass as feedstock for a bioenergy and bioproducts industry: the technical feasibility of a billion-ton annual supply*. Oak Ridge National Laboratory: 2005.
9. Stevanovic, T., Chemical Composition and Properties of Wood. In *Lignocellulosic Fibers and Wood Handbook*, 2016.
10. Nitsos, C. K.; Choli-Papadopoulou, T.; Matis, K. A.; Triantafyllidis, K. S., Optimization of Hydrothermal Pretreatment of Hardwood and Softwood Lignocellulosic Residues for Selective Hemicellulose Recovery and Improved Cellulose Enzymatic Hydrolysis. *ACS Sustainable Chemistry & Engineering* **2016,** *4* (9), 4529-4544.
11. Álvarez, C.; Reyes-Sosa, F. M.; Díez, B., Enzymatic hydrolysis of biomass from wood. *Microbial Biotechnology* **2016,** *9* (2), 149-156.
12. Anwar, Z.; Gulfraz, M.; Irshad, M., Agro-industrial lignocellulosic biomass a key to unlock the future bio-energy: A brief review. *Journal of Radiation Research and Applied Sciences* **2014,** *7* (2), 163-173.
13. Kishimoto, T.; Chiba, W.; Saito, K.; Fukushima, K.; Uraki, Y.; Ubukata, M., Influence of Syringyl to Guaiacyl Ratio on the Structure of Natural and Synthetic Lignins. *Journal of Agricultural and Food Chemistry* **2010,** *58* (2), 895-901.
14. Wagner, A.; Tobimatsu, Y.; Phillips, L.; Flint, H.; Geddes, B.; Lu, F.; Ralph, J., Syringyl lignin production in conifers: Proof of concept in a Pine tracheary element system. *Proceedings of the National Academy of Sciences* **2015,** *112* (19), 6218.

15. Nitsos, C.; Rova, U.; Christakopoulos, P., Organosolv fractionation of softwood biomass for biofuel and biorefinery applications. *Energies* **2017,** *11* (1), 50.
16. Rajan, K.; Carrier, D. J., Effect of dilute acid pretreatment conditions and washing on the production of inhibitors and on recovery of sugars during wheat straw enzymatic hydrolysis. *Biomass and Bioenergy* **2014,** *62*, 222-227.
17. Mes-Hartree, M.; Saddler, J. N. J. B. L., The nature of inhibitory materials present in pretreated lignocellulosic substrates which inhibit the enzymatic hydrolysis of cellulose. **1983,** *5* (8), 531-536.
18. Yang, B.; Wyman, C. E., Pretreatment: the key to unlocking low-cost cellulosic ethanol. *Biofuels, Bioprod. Biorefin.* **2008,** *2* (1), 26-40.
19. Shuai, L.; Yang, Q.; Zhu, J.; Lu, F.; Weimer, P.; Ralph, J.; Pan, X., Comparative study of SPORL and dilute-acid pretreatments of spruce for cellulosic ethanol production. *Biores. Tech.* **2010,** *101*, 3106-3114.
20. Normark, M.; Winestrand, S.; Lestander, T. A.; Jönsson, L. J., Analysis, pretreatment and enzymatic saccharification of different fractions of Scots pine. *BMC Biotechnology* **2014,** *14* (1), 20.
21. Zhang, L.; Pu, Y.; Cort, J. R.; Ragauskas, A. J.; Yang, B., Revealing the Molecular Structural Transformation of Hardwood and Softwood in Dilute Acid Flowthrough Pretreatment. *ACS Sustainable Chemistry & Engineering* **2016,** *4* (12), 6618-6628.
22. Nguyen, Q.; Tucker, M.; A. Keller, F.; P. Eddy, F., *Two-Stage Dilute-Acid Pretreatment of Softwoods*. 2000; Vol. 84-86, p 561-76.
23. Sun, Z.; Fridrich, B.; de Santi, A.; Elangovan, S.; Barta, K., Bright Side of Lignin Depolymerization: Toward New Platform Chemicals. *Chemical Reviews* **2018,** *118* (2), 614-678.
24. Szijártó, N.; Siika-aho, M.; Tenkanen, M.; Alapuranen, M.; Vehmaanperä, J.; Réczey, K.; Viikari, L., Hydrolysis of amorphous and crystalline cellulose by heterologously produced cellulases of Melanocarpus albomyces. *Journal of Biotechnology* **2008,** *136* (3), 140-147.
25. Hall, M.; Bansal, P.; Lee, J. H.; Realff, M. J.; Bommarius, A. S., Cellulose crystallinity – a key predictor of the enzymatic hydrolysis rate. *The FEBS Journal* **2010,** *277* (6), 1571-1582.
26. Sathitsuksanoh, N.; Zhu, Z.; Zhang, Y.-H. P., Cellulose solvent-based pretreatment for corn stover and avicel: concentrated phosphoric acid versus ionic liquid [BMIM]Cl. *Cellulose* **2012,** *19* (4), 1161-1172.
27. Satari, B.; Karimi, K.; Kumar, R., Cellulose solvent-based pretreatment for enhanced second-generation biofuel production: a review. *Sustainable Energy & Fuels* **2019,** *3* (1), 11-62.
28. Siripong, P.; Duangporn, P.; Takata, E.; Tsutsumi, Y., Phosphoric acid pretreatment of Achyranthes aspera and Sida acuta weed biomass to improve enzymatic hydrolysis. *Biores. technol.* **2016,** *203*, 303-308.
29. Nair, R.; Lundin, M.; Lennartsson, P.; Taherzadeh, M., Optimizing dilute phosphoric acid pretreatment of wheat straw in the laboratory and in a demonstration plant for ethanol and edible fungal biomass production using Neurospora intermedia. *J. Chem. Technol. Biotechnol.* **2017,** *92* (6), 1256-1265.

30. Wu, W.; Rondon, V.; Weeks, K.; Pullammanappallil, P.; Ingram, L.; Shanmugam, K., Phosphoric acid based pretreatment of switchgrass and fermentation of entire slurry to ethanol using a simplified process. *Biores. Technol.* **2018,** *251*, 171-180.
31. Yu, H.; Xiao, W.; Han, L.; Huang, G., Characterization of mechanical pulverization/phosphoric acid pretreatment of corn stover for enzymatic hydrolysis. *Biores. Technol.* **2019,** *282*, 69-74.
32. Hewetson, B.; Zhang, X.; Mosier, N., Enhanced acid-catalyzed biomass conversion to hydroxymethylfurfural following cellulose solvent-and organic solvent-based lignocellulosic fractionation pretreatment. *Energy & Fuels* **2016,** *30* (11), 9975-9977.
33. Li, H.; Kim, N.-J.; Jiang, M.; Kang, J. W.; Chang, H. N., Simultaneous saccharification and fermentation of lignocellulosic residues pretreated with phosphoric acid–acetone for bioethanol production. *Bioresource Technology* **2009,** *100* (13), 3245-3251.
34. Sathitsuksanoh, N.; Zhu, Z.; Wi, S.; Percival Zhang, Y. H., Cellulose solvent-based biomass pretreatment breaks highly ordered hydrogen bonds in cellulose fibers of switchgrass. *Biotechnology and Bioengineering* **2011,** *108* (3), 521-529.
35. Moxley, G.; Zhu, Z.; Zhang, Y. H. P., Efficient Sugar Release by the Cellulose Solvent-Based Lignocellulose Fractionation Technology and Enzymatic Cellulose Hydrolysis. *Journal of Agricultural and Food Chemistry* **2008,** *56* (17), 7885-7890.
36. Sathitsuksanoh, N.; Sawant, M.; Truong, Q.; Tan, J.; Canlas, C. G.; Sun, N.; Zhang, W.; Renneckar, S.; Prasomsri, T.; Shi, J.; Çetinkol, Ö. P.; Singh, S.; Simmons, B. A.; George, A., How Alkyl Chain Length of Alcohols Affects Lignin Fractionation and Ionic Liquid Recycle During Lignocellulose Pretreatment. *BioEnerg. Res.* **2015,** *8* (3), 973-981.
37. McDonald, W. F.; Bathula, N. V. K.; Bowyer, M.; Kiser, B.; Srinivasan, V.; Tenlep, L.; Walker, B.-A. System and method for treatment of biomass for the production of biofuels and biochemicals. 2017.
38. Sathitsuksanoh, N.; Zhu, Z.; Wi, S.; Zhang, Y.-H. P., Cellulose solvent based biomass pretreatment breaks highly ordered hydrogen bonds in cellulose fibers of switchgrass. *Biotechnol. Bioeng.* **2011,** *108* (3), 521–529.
39. Sathitsuksanoh, N.; Zhu, Z.; Zhang, Y.-H. P., Cellulose Solvent-Based Pretreatment for Corn Stover and Avicel: Concentrated Phosphoric Acid versus Ionic Liquid [BMIM]Cl. *Cellulose* **2012,** *DOI: 10.1007/s10570-012-9719-z*.
40. Rollin, J. A.; Zhu, Z.; Sathitsuksanoh, N.; Zhang, Y. H. P., Increasing cellulose accessibility is more important than removing lignin: A comparison of cellulose solvent-based lignocellulose fractionation and soaking in aqueous ammonia. *Biotechnol. bioeng.* **2011,** *108* (1), 22-30.
41. Sathitsuksanoh, N.; Zhu, Z.; Templeton, N.; Rollin, J. A.; Harvey, S. P.; Zhang, Y. H. P., Saccharification of a Potential Bioenergy Crop, Phragmites australis (Common Reed), by Lignocellulose Fractionation Followed by Enzymatic Hydrolysis at Decreased Cellulase Loadings. *Industrial & Engineering Chemistry Research* **2009,** *48* (13), 6441-6447.
42. Sluiter, A.; Hames, B.; Ruiz, R.; Scarlata, C.; Sluiter, J.; Templeton, D.; Crocker, D., Determination of structural carbohydrates and lignin in biomass. Laboratory

Analytical Procedure (LAP). Avalable: http://www.nrel.gov/biomass/pdfs/42618.pdf. Accessed 2013 July 7. In *Technical Report. NREL/TP-510-42618.*, 2011.
43. Sluiter, A.; Hames, B.; Ruiz, R.; Scarlata, C.; Sluiter, J.; Templeton, D., Determination of ash in biomass. Laboratory Analytical Procedure (LAP). . In *Technical Report. NREL/TP-510-42622.*, 2008; pp 1-5.
44. Zhu, Z.; Sathitsuksanoh, N.; Vinzant, T.; Schell, D. J.; McMillan, J. D.; Zhang, Y. H. P., Comparative study of corn stover pretreated by dilute acid and cellulose solvent-based lignocellulose fractionation: Enzymatic hydrolysis, supramolecular structure, and substrate accessibility. *Biotechnol. bioeng.* **2009,** *103* (4), 715-724.
45. Hong, J.; Ye, X.; Wang, Y.; Zhang, Y.-H. P., Bioseparation of recombinant cellulose-binding module-proteins by affinity adsorption on an ultra-high-capacity cellulosic adsorbent. *Anal. Chim. Acta* **2008,** *621* (2), 193-199.
46. Park, S.; Baker, J. O.; Himmel, M. E.; Parilla, P. A.; Johnson, D. K., Cellulose crystallinity index: measurement techniques and their impact on interpreting cellulase performance. *Biotechnology for Biofuels* **2010,** *3*, 10-10.
47. Kim, H.; Ralph, J., Solution-state 2D NMR of ball-milled plant cell wall gels in DMSO-d6/pyridine-d5. *Org. Biomol. Chem.* **2010,** *8* (3), 576-591.
48. Mansfield, S. D.; Kim, H.; Lu, F.; Ralph, J., Whole plant cell wall characterization using solution-state 2D NMR. *Nat. Protoc.* **2012,** *7* (9), 1579-1589.
49. Sathitsuksanoh, N.; Holtman, K. M.; Yelle, D. J.; Morgan, T.; Stavila, V.; Pelton, J.; Blanch, H.; Simmons, B. A.; George, A., Lignin fate and characterization during ionic liquid biomass pretreatment for renewable chemicals and fuels production. *Green Chem.* **2014,** *16* (3), 1236-1247.
50. Cheng, K.; Sorek, H.; Zimmermann, H.; Wemmer, D. E.; Pauly, M., Solution-State 2D NMR Spectroscopy of Plant Cell Walls Enabled by a Dimethylsulfoxide-d 6/1-Ethyl-3-methylimidazolium Acetate Solvent. *Anal chem.* **2013,** *85* (6), 3213-3221.
51. Heikkinen, S.; Toikka, M. M.; Karhunen, P. T.; Kilpeläinen, I. A., Quantitative 2D HSQC (Q-HSQC) via suppression of J-dependence of polarization transfer in NMR spectroscopy: application to wood lignin. *Journal of the American Chemical Society* **2003,** *125* (14), 4362-4367.
52. Yelle, D. J.; Ralph, J.; Frihart, C. R., Characterization of nonderivatized plant cell walls using high-resolution solution-state NMR spectroscopy. *Magn. Reson. Chem.* **2008,** *46* (6), 508-517.
53. Biswas, R.; Teller, P. J.; Ahring, B. K., Pretreatment of forest residues of Douglas fir by wet explosion for enhanced enzymatic saccharification. *Bioresource Technology* **2015,** *192*, 46-53.
54. Yang, B.; Wyman, C. E., Pretreatment: the key to unlocking low-cost cellulosic ethanol. *Biofuels, Bioprod. Bioref.* **2008,** *2* (1), 26-40.
55. Funaoka, M.; Kako, T.; Abe, I., Condensation of lignin during heating of wood. *Wood Science Technology* **1990,** *24* (3), 277-288.
56. Fujii, T.; Fang, X.; Inoue, H.; Murakami, K.; Sawayama, S., Enzymatic hydrolyzing performance of Acremonium cellulolyticus and Trichoderma reesei against three lignocellulosic materials. *Biotechnol. Biofuel.* **2009,** *2* (1), 24.
57. Rana, D.; Rana, V.; Ahring, B. K., Producing high sugar concentrations from loblolly pine using wet explosion pretreatment. *Biores. Technol.* **2012,** *121* (Supplement C), 61-67.

58. Sannigrahi, P.; Miller, S. J.; Ragauskas, A. J., Effects of organosolv pretreatment and enzymatic hydrolysis on cellulose structure and crystallinity in Loblolly pine. *Carbohyd. Res.* **2010,** *345* (7), 965-970.
59. Sheldon, R. A., The e Factor: Fifteen years on. *Green Chemistry* **2007,** *9* (12), 1273-1283.
60. Sheldon, R. A.; Sanders, J. P. M., Toward concise metrics for the production of chemicals from renewable biomass. *Catalysis Today* **2015,** *239*, 3-6.
61. Overend, R. P.; Chornet, E.; Gascoigne, J. A., Fractionation of Lignocellulosics by Steam-Aqueous Pretreatments [and Discussion]. *Philosophical Transactions of the Royal Society of London. Series A, Mathematical and Physical Sciences* **1987,** *321* (1561), 523-536.
62. Klein-Marcuschamer, D.; Oleskowicz-Popiel, P.; Simmons, B. A.; Blanch, H. W., Technoeconomic analysis of biofuels: A wiki-based platform for lignocellulosic biorefineries. *Biomass Bioenergy* **2010,** *34* (12), 1914-1921.
63. Klein-Marcuschamer, D.; Simmons, B.; Blanch, H., Techno-economic analysis of a lignocellulosic ethanol biorefinery with ionic liquid pre-treatment. *Biofuels, Bioprod. Bioref.* **2011**, DOI: 10.1002/bbb.303.
64. Amin, M. I.; Ali, M. M.; Kamal, H. M.; Youssef, A. M.; Akl, M. A., Recovery of high grade phosphoric acid from wet process acid by solvent extraction with aliphatic alcohols. *Hydrometallurgy* **2010,** *105* (1), 115-119.
65. Assuncao, M. C.; Cote, G.; Andre, M.; Halleux, H.; Chagnes, A., Phosphoric acid recovery from concentrated aqueous feeds by a mixture of di-isopropyl ether (DiPE) and tri-n-butylphosphate (TBP): extraction data and modelling. *RSC Advances* **2017,** *7* (12), 6922-6930.
66. Kim, J.-Y.; Shin, C.-H.; Choi, H.; Bae, W., Recovery of phosphoric acid from mixed waste acids of semiconductor industry by diffusion dialysis and vacuum distillation. *Separation and Purification Technology* **2012,** *90*, 64-68.
67. Liu, Y.; Chen, J., Phosphorus Cycle. In *Encyclopedia of Ecology*, Jørgensen, S. E.; Fath, B. D., Eds. Academic Press: Oxford, 2008; pp 2715-2724.
68. Dutta, T.; Papa, G.; Wang, E.; Sun, J.; Isern, N. G.; Cort, J. R.; Simmons, B. A.; Singh, S., Characterization of Lignin Streams during Bionic Liquid-Based Pretreatment from Grass, Hardwood, and Softwood. *ACS Sustainable Chemistry & Engineering* **2018,** *6* (3), 3079-3090.
69. Trinh, L. T. P.; Lee, Y. J.; Lee, J.-W.; Lee, H.-J., Characterization of ionic liquid pretreatment and the bioconversion of pretreated mixed softwood biomass. *Biomass Bioenergy* **2015,** *81*, 1-8.
70. Gschwend, F.; Chambon, C.; Biedka, M.; Brandt-Talbot, A.; Fennell, P.; Hallett, J., Quantitative glucose release from softwood after pretreatment with low-cost ionic liquids. *Green Chem.* **2019,** *21* (3), 692-703.
71. Mabee, W. E.; Gregg, D. J.; Arato, C.; Berlin, A.; Bura, R.; Gilkes, N.; Mirochnik, O.; Pan, X.; Pye, E. K.; Saddler, J. N., Updates on Softwood-to-Ethanol Process Development. *Appl. Biochem. Biotechnol.* **2006,** *129–132*, 55-70.
72. Takada, M.; Chandra, R. P.; Saddler, J. N., The influence of lignin migration and relocation during steam pretreatment on the enzymatic hydrolysis of softwood and corn stover biomass substrates. *Biotechnology and Bioengineering* **2019,** *116* (11), 2864-2873.

73. Ewanick, S. M.; Bura, R.; Saddler, J. N., Acid catalyzed steam pretreatment of lodgepole pine and subsequent enzymatic hydrolysis and fermentation to ethanol. *Biotechnol. Bioeng.* **2007,** *98* (4), 737-746.
74. Nakagame, S.; Chandra, R. P.; Kadla, J. F.; Saddler, J. N., The isolation, characterization and effect of lignin isolated from steam pretreated Douglas-fir on the enzymatic hydrolysis of cellulose. *Bioresour Technol* **2011,** *102* (6), 4507-17.
75. Yang, B.; Boussaid, A.; Mansfield, S. D.; Gregg, D. J.; Saddler, J. N., Fast and efficient alkaline peroxide treatment to enhance the enzymatic digestibility of steam-exploded softwood substrates. *Biotechnol Bioeng* **2002,** *77* (6), 678-84.
76. Pan, X.; Zhang, X.; Gregg, D. J.; Saddler, J. N., Enhanced Enzymatic Hydrolysis of Steam-Exploded Douglas Fir Wood by Alkali-Oxygen Post-treatment. *Appl. Biochem. Biotechnol.* **2004,** *115* (1-3), 1103-1114.
77. Tarasov, D.; Leitch, M.; Fatehi, P., Lignin-carbohydrate complexes: properties, applications, analyses, and methods of extraction: a review. *Biotechnology for biofuels* **2018,** *11*, 269-269.
78. Zhang, J.; Zhang, J.; Lin, L.; Chen, T.; Zhang, J.; Liu, S.; Li, Z.; Ouyang, P., Dissolution of Microcrystalline Cellulose in Phosphoric Acid—Molecular Changes and Kinetics. *Molecules* **2009,** *14* (12), 5027-5041.
79. Zhang, Y.-H. P.; Cui, J.; Lynd, L. R.; Kuang, L. R., A transition from cellulose swelling to cellulose dissolution by o-phosphoric acid: evidence from enzymatic hydrolysis and supramolecular structure. *Biomacromolecules* **2006,** *7* (2), 644-648.
80. Kang, P.; Qin, W.; Zheng, Z.-M.; Dong, C.-Q.; Yang, Y.-P., Theoretical study on the mechanisms of cellulose dissolution and precipitation in the phosphoric acid–acetone process. *Carbohydrate Polymers* **2012,** *90* (4), 1771-1778.
81. Wiman, M.; Dienes, D.; Hansen, M. A. T.; van der Meulen, T.; Zacchi, G.; Lidén, G., Cellulose accessibility determines the rate of enzymatic hydrolysis of steam-pretreated spruce. *Bioresource Technology* **2012,** *126*, 208-215.
82. Liimatainen, H.; Sirviö, J.; Haapala, A.; Hormi, O.; Niinimäki, J., Characterization of highly accessible cellulose microfibers generated by wet stirred media milling. *Carbohydrate Polymers* **2011,** *83* (4), 2005-2010.
83. Sathitsuksanoh, N.; George, A.; Zhang, Y.-H. P., New lignocellulose pretreatments using cellulose solvents: a review. *Journal of Chemical Technology and Biotechnology* **2013,** *88* (2), 169-180.
84. Hong, J.; Ye, X.; Zhang, Y. H. P., Quantitative Determination of Cellulose Accessibility to Cellulase Based on Adsorption of a Nonhydrolytic Fusion Protein Containing CBM and GFP with Its Applications. *Langmuir* **2007,** *23* (25), 12535-12540.
85. Hong, J.; Ye, X.; Zhang, Y., Quantitative determination of cellulose accessibility to cellulase based on adsorption of a nonhydrolytic fusion protein containing CBM and GFP with its applications. *Langmuir* **2007,** *23* (25), 12535-12540.
86. Zhang, Y.-H. P.; Lynd, L. R., Toward an aggregated understanding of enzymatic hydrolysis of cellulose: Noncomplexed cellulase systems. *Biotechnol. Bioeng.* **2004,** *88*, 797-824.
87. Rollin, J. A.; Zhu, Z.; Sathitsuksanoh, N.; Zhang, Y.-H. P., Increasing cellulose accessibility is more important than removing lignin: A comparison of cellulose solvent-based lignocellulose fractionation and soaking in aqueous ammonia. *Biotechnol. Bioeng.* **2011,** *108* (1), 22-30.

88. Sathitsuksanoh, N.; Zhu, Z.; Zhang, Y.-H. P., Cellulose solvent- and organic solvent-based lignocellulose fractionation enabled efficient sugar release from a variety of lignocellulosic feedstocks. *Biores. Technol.* **2012,** *117*, 228-233.
89. Marchessault, R. H.; Liang, C. Y., The infrared spectra of crystalline polysaccharides. VIII. Xylans. *Journal of Polymer Science* **1962,** *59* (168), 357-378.
90. Faix, O., Fourier Transform Infrared Spectroscopy. In *Methods in Lignin Chemistry*, Lin, S. Y.; Dence, C. W., Eds. Springer Berlin Heidelberg: Berlin, Heidelberg, 1992; pp 83-109.
91. Schultz, T. P.; Glasser, W. G., Quantitative structural analysis of lignin by diffuse reflectance fourier transform infrared spectrometry. *Holzforschung* **1986,** *40(suppl.)*, 37-44.
92. Sills, D. L.; Gossett, J. M., Using FTIR to predict saccharification from enzymatic hydrolysis of alkali-pretreated biomasses. *Biotechnol. Bioeng.* **2012,** *109* (2), 353-362.
93. Fan, M.; Dai, D.; Huang, B., Fourier transform infrared spectroscopy for natural fibres. In *Fourier Transform-Materials Analysis*, InTech: 2012.
94. Brownleader, M. D.; Harborne, J. B.; Dey, P. M., 3 - Carbohydrate Metabolism: Primary Metabolism of Monosaccharides. In *Plant Biochemistry*, Dey, P. M.; Harborne, J. B., Eds. Academic Press: London, 1997; pp 111-141.
95. Kamide, K.; Okajima, K., Determination of Distribution of O-Acetyl Group in Trihydric Alcohol Units of Cellulose Acetate by Carbon-13 Nuclear Magnetic Resonance Analysis. *Polymer Journal* **1981,** *13* (2), 127-133.
96. Marchessault, R. H.; Liang, C. Y., The infrared spectra of crystalline polysaccharides. VIII. Xylans. *J. Polym. Sci.* **1962,** *59* (168), 357-378.
97. Marchessault, R. H., Application of infra-red spectroscopy to cellulose and wood polysaccharides. *Pure Appl. Chem.* **1962,** *5* (1-2), 107-130.
98. Schultz, T. P.; Glasser, W. G., Quantitative structural analysis of lignin by diffuse reflectance fourier transform infrared spectrometry. *Holzforschung* **1986,** *40* (suppl.), 37-44.
99. Jia, X.; Chen, Y.; Shi, C.; Ye, Y.; Wang, P.; Zeng, X.; Wu, T., Preparation and Characterization of Cellulose Regenerated from Phosphoric Acid. *Journal of Agricultural and Food Chemistry* **2013,** *61* (50), 12405-12414.
100. Wada, M.; Ike, M.; Tokuyasu, K., Enzymatic hydrolysis of cellulose I is greatly accelerated via its conversion to the cellulose II hydrate form. *Polymer Degradation and Stability* **2010,** *95* (4), 543-548.
101. Sathitsuksanoh, N.; Renneckar, S., Characterization Methods and Techniques. In *Introduction to Renewable Biomaterials: First Principles and Concepts*, Ayoub, A. S.; Lucia, L. A., Eds. pp 107-140.
102. Park, S.; Baker, J. O.; Himmel, M. E.; Parilla, P. A.; Johnson, D. K., Cellulose crystallinity index: measurement techniques and their impact on interpreting cellulase performance. *Biotechnol. biofuels* **2010,** *3* (1), 1.
103. Park, S.; Johnson, D. K.; Ishizawa, C. I.; Parilla, P. A.; Davis, M. F., Measuring the crystallinity index of cellulose by solid state 13C nuclear magnetic resonance. *Cellulose* **2009,** *16* (4), 641-647.
104. Park, S.; Baker, J. O.; Himmel, M. E.; Parilla, P. A.; Johnson, D. K., Cellulose crystallinity index: measurement techniques and their impact on interpreting cellulase performance. *Biotechnology for Biofuels* **2010,** *3* (1), 10.

105. Gao, S.; You, C.; Renneckar, S.; Bao, J.; Zhang, Y.-H. P., New insights into enzymatic hydrolysis of heterogeneous cellulose by using carbohydrate-binding module 3 containing GFP and carbohydrate-binding module 17 containing CFP. *Biotechnology for biofuels* **2014,** *7* (1), 24-24.
106. Kim, H.; Ralph, J., Solution-state 2D NMR of ball-milled plant cell wall gels in DMSO-d6/pyridine-d5. *Organic & Biomolecular Chemistry* **2010,** *8* (3), 576-591.
107. Mansfield, S. D.; Kim, H.; Lu, F.; Ralph, J., Whole plant cell wall characterization using solution-state 2D NMR. *Nat. Protocols* **2012,** *7* (9), 1579-1589.
108. Kim, H.; Ralph, J.; Akiyama, T., Solution-state 2D NMR of ball-milled plant cell wall gels in DMSO-d6. *BioEnerg. Res.* **2008,** *1* (1), 56-66.
109. Kim, H.; Ralph, J., A gel-state 2D-NMR method for plant cell wall profiling and analysis: a model study with the amorphous cellulose and xylan from ball-milled cotton linters. *Rsc Adv.* **2014,** *4* (15), 7549-7560.
110. Käldström, M.; Meine, N.; Farès, C.; Schüth, F.; Rinaldi, R., Deciphering 'water-soluble lignocellulose'obtained by mechanocatalysis: new insights into the chemical processes leading to deep depolymerization. *Green Chem.* **2014,** *16* (7), 3528-3538.
111. Puls, J. In *Chemistry and biochemistry of hemicelluloses: Relationship between hemicellulose structure and enzymes required for hydrolysis*, Macromol. Symp., Wiley Online Library: 1997; pp 183-196.
112. Willför, S.; Sundberg, K.; Tenkanen, M.; Holmbom, B., Spruce-derived mannans–A potential raw material for hydrocolloids and novel advanced natural materials. *Carbohydr. Polym.* **2008,** *72* (2), 197-210.
113. Sette, M.; Lange, H.; Crestini, C., Quantitative HSQC analyses of lignin: a practical comparison. *Comput. Struct. Biotechnol. J.* **2013,** *6* (7), 1-7.
114. Sette, M.; Wechselberger, R.; Crestini, C., Elucidation of lignin structure by quantitative 2D NMR. *Chem. Eur. J.* **2011,** *17* (34), 9529-9535.
115. Dutta, T.; Papa, G.; Wang, E.; Sun, J.; Isern, N. G.; Cort, J. R.; Simmons, B. A.; Singh, S., Characterization of lignin streams during bionic liquid-based pretreatment from grass, hardwood, and softwood. *ACS Sustainable Chem. Eng.* **2018,** *6* (3), 3079-3090.
116. Li, N.; Li, Y.; Yoo, C. G.; Yang, X.; Lin, X.; Ralph, J.; Pan, X., An uncondensed lignin depolymerized in the solid state and isolated from lignocellulosic biomass: a mechanistic study. *Green Chem.* **2018,** *20* (18), 4224-4235.
117. Parthasarathi, R.; Romero, R. A.; Redondo, A.; Gnanakaran, S., Theoretical study of the remarkably diverse linkages in lignin. *J. Phys. Chem. Lett.* **2011,** *2* (20), 2660-2666.
118. Wen, J.-L.; Sun, S.-N.; Yuan, T.-Q.; Xu, F.; Sun, R.-C., Fractionation of bamboo culms by autohydrolysis, organosolv delignification and extended delignification: Understanding the fundamental chemistry of the lignin during the integrated process. *Biores. Technol.* **2013,** *150*, 278-286.
119. Hossain, M. A.; Phung, T. K.; Rahaman, M. S.; Tulaphol, S.; Jasinski, J. B.; Sathitsuksanoh, N., Catalytic cleavage of the β-O-4 aryl ether bonds of lignin model compounds by Ru/C catalyst. *Appl. Catal., A* **2019,** *582*, 117100.
120. Liu, L.-Y.; Cho, M.; Sathitsuksanoh, N.; Chowdhury, S.; Renneckar, S., Uniform Chemical Functionality of Technical Lignin Using Ethylene Carbonate for

Hydroxyethylation and Subsequent Greener Esterification. *ACS Sustainable Chem. Eng.* **2018,** *6* (9), 12251-12260.
121. Alonso, D. M.; Hakim, S. H.; Zhou, S.; Won, W.; Hosseinaei, O.; Tao, J.; Garcia-Negron, V.; Motagamwala, A. H.; Mellmer, M. A.; Huang, K., Increasing the revenue from lignocellulosic biomass: Maximizing feedstock utilization. *Sci. Adv.* **2017,** *3* (5), e1603301.

Figure 1. Hydrolysis of H_3PO_4-pretreated yellow pine samples (A) and Douglas fir (B) at 5 and 15 FPU/g glucan.

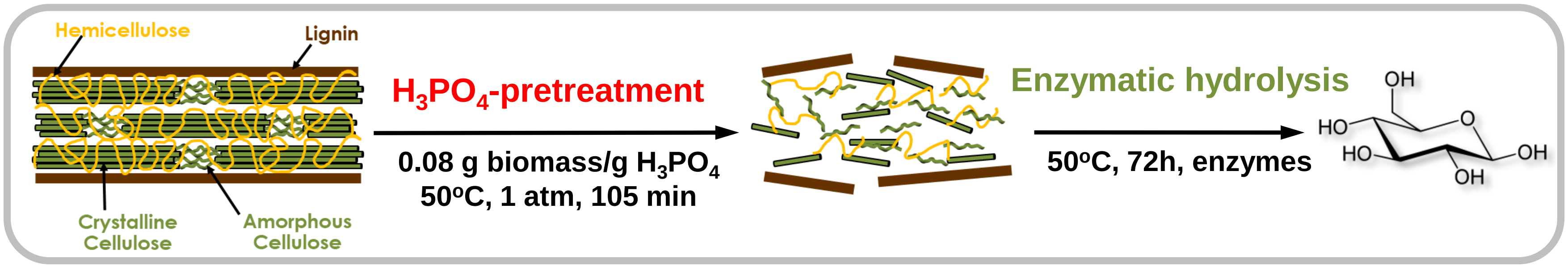

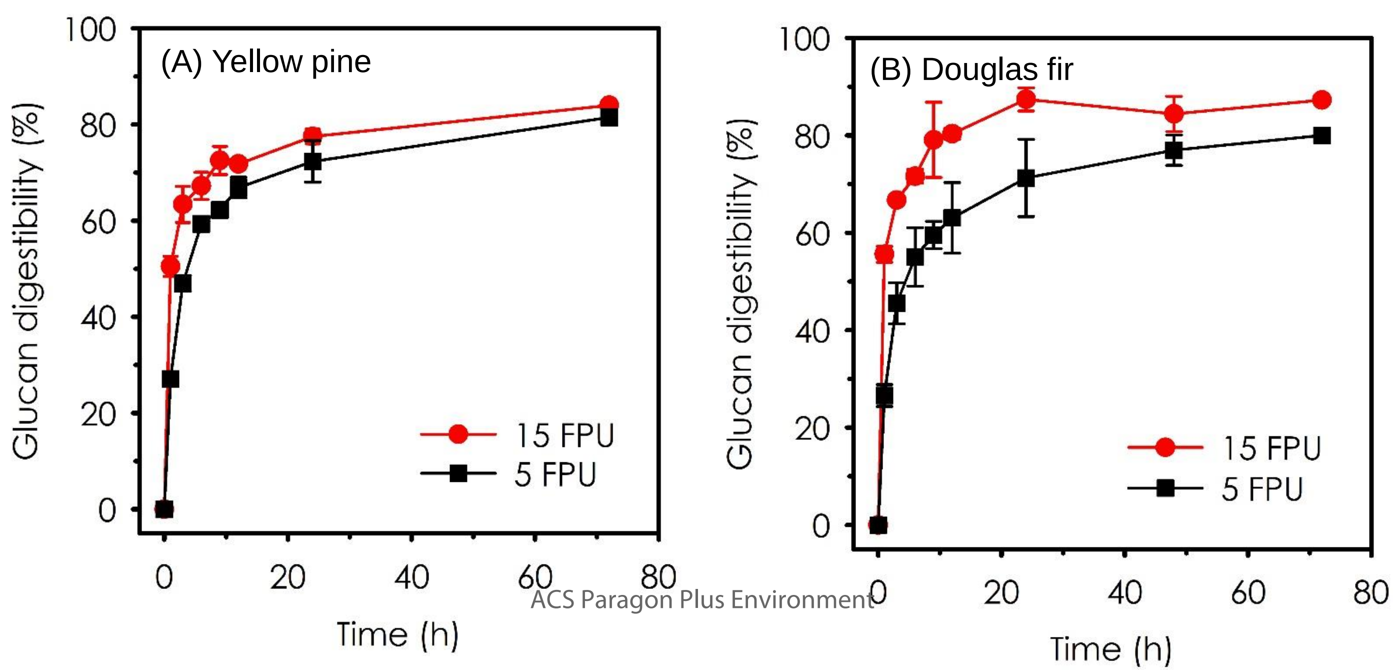

Figure 2. Mass balance of H_3PO_4-pretreated yellow pine (A) and H_3PO_4-pretreated Douglas fir (B) at 5 FPU/ g glucan.

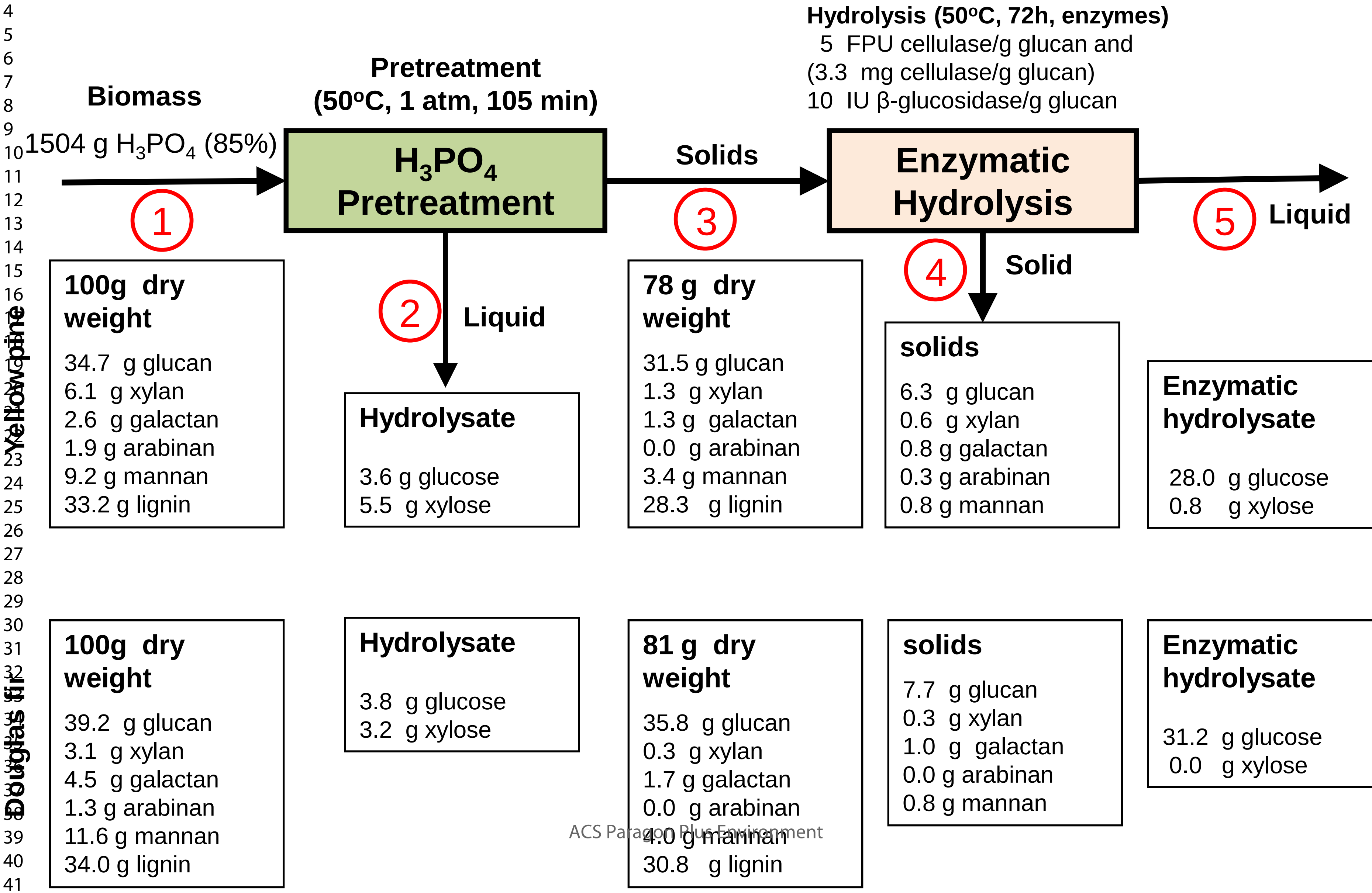

Figure 3. SEM micrographs of untreated and pretreated yellow pine (A and C), as well as untreated and pretreated Douglas fir (B and D).

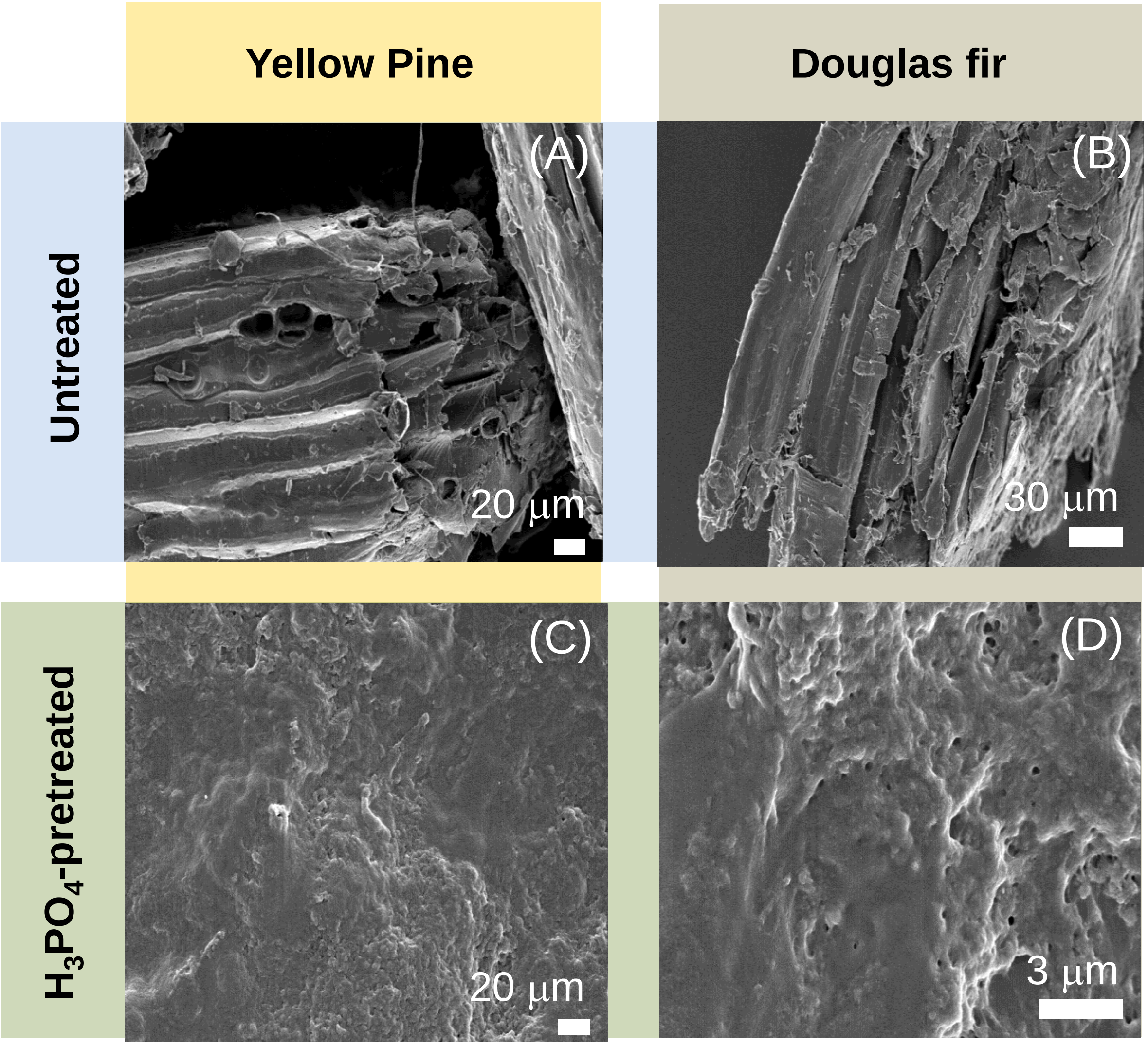

Figure 4 Total surface accessibility to cellulase (TSAC), cellulose accessibility to cellulase (CAC), and glucan digestibility after 72 h with 5 FPU of cellulase and 10 units of β-glucosidase per gram of glucan.

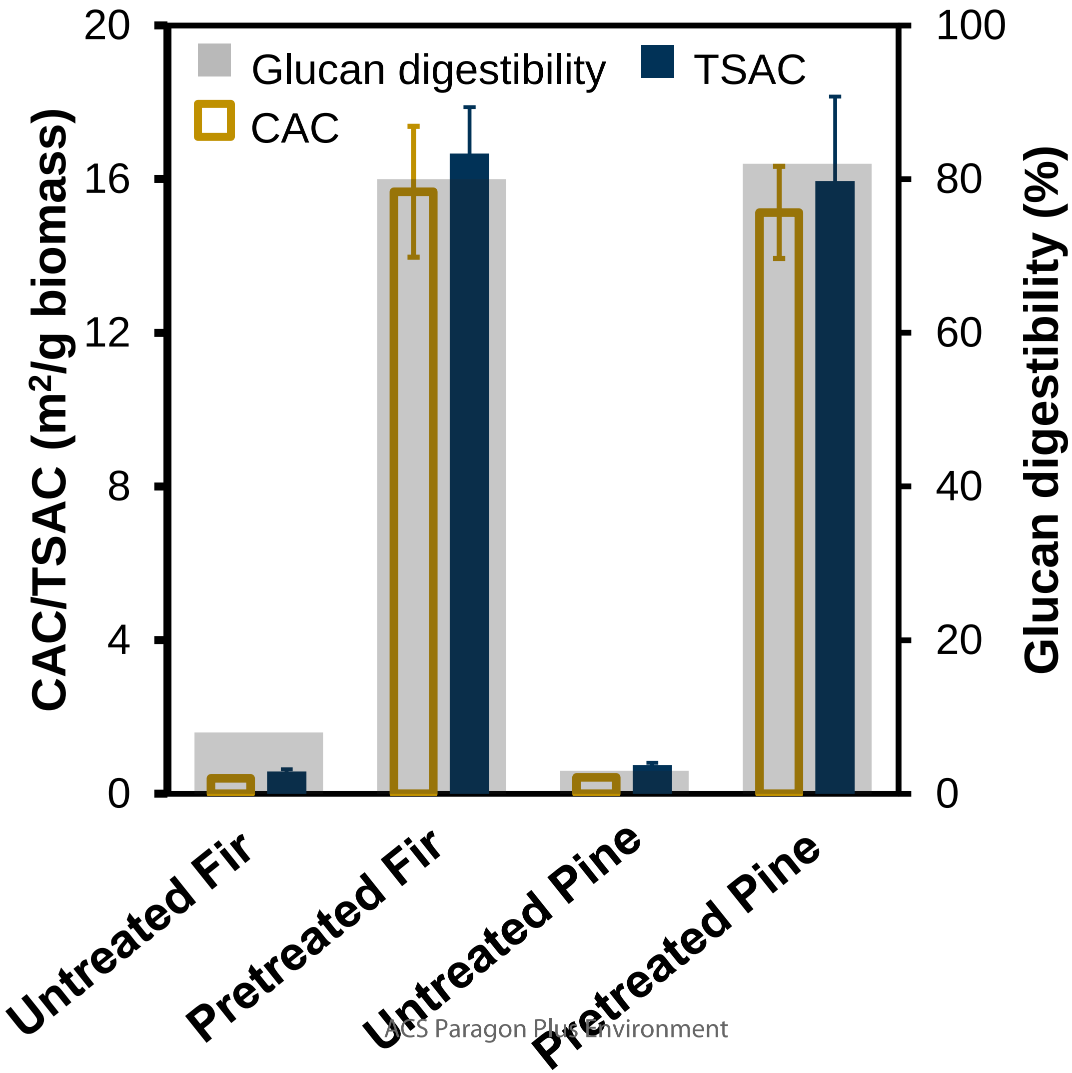

Figure 5. FT-IR spectra of yellow pine and Douglas fir before and after H_3PO_4 pretreatment.

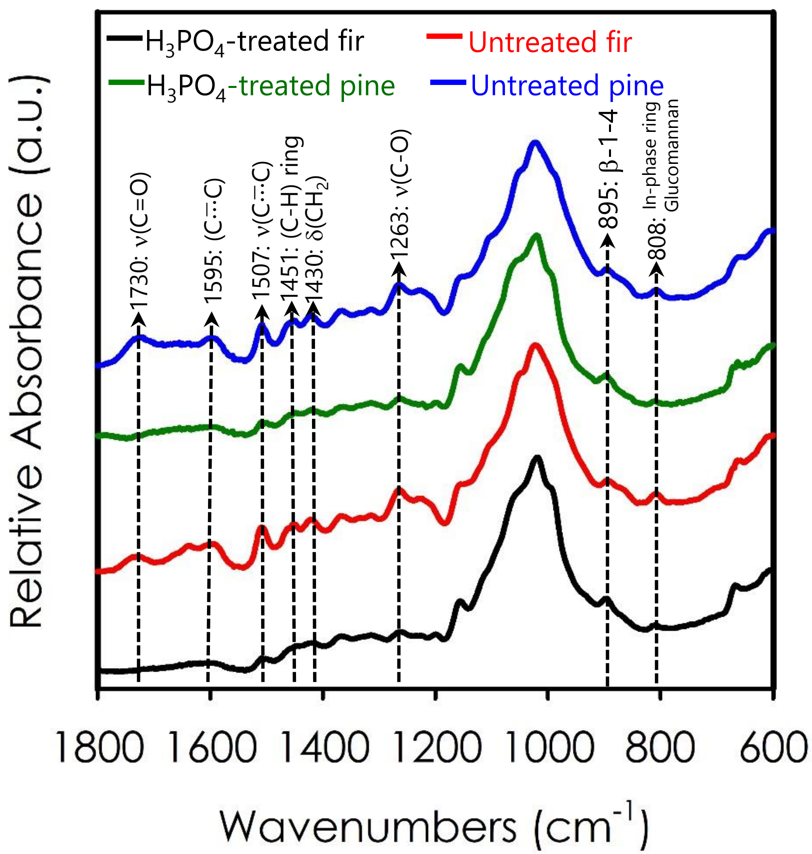

Figure 6. CP/MAS ^{13}C-NMR spectra of yellow pine and Douglas fir samples before and after H_3PO_4 pretreatment

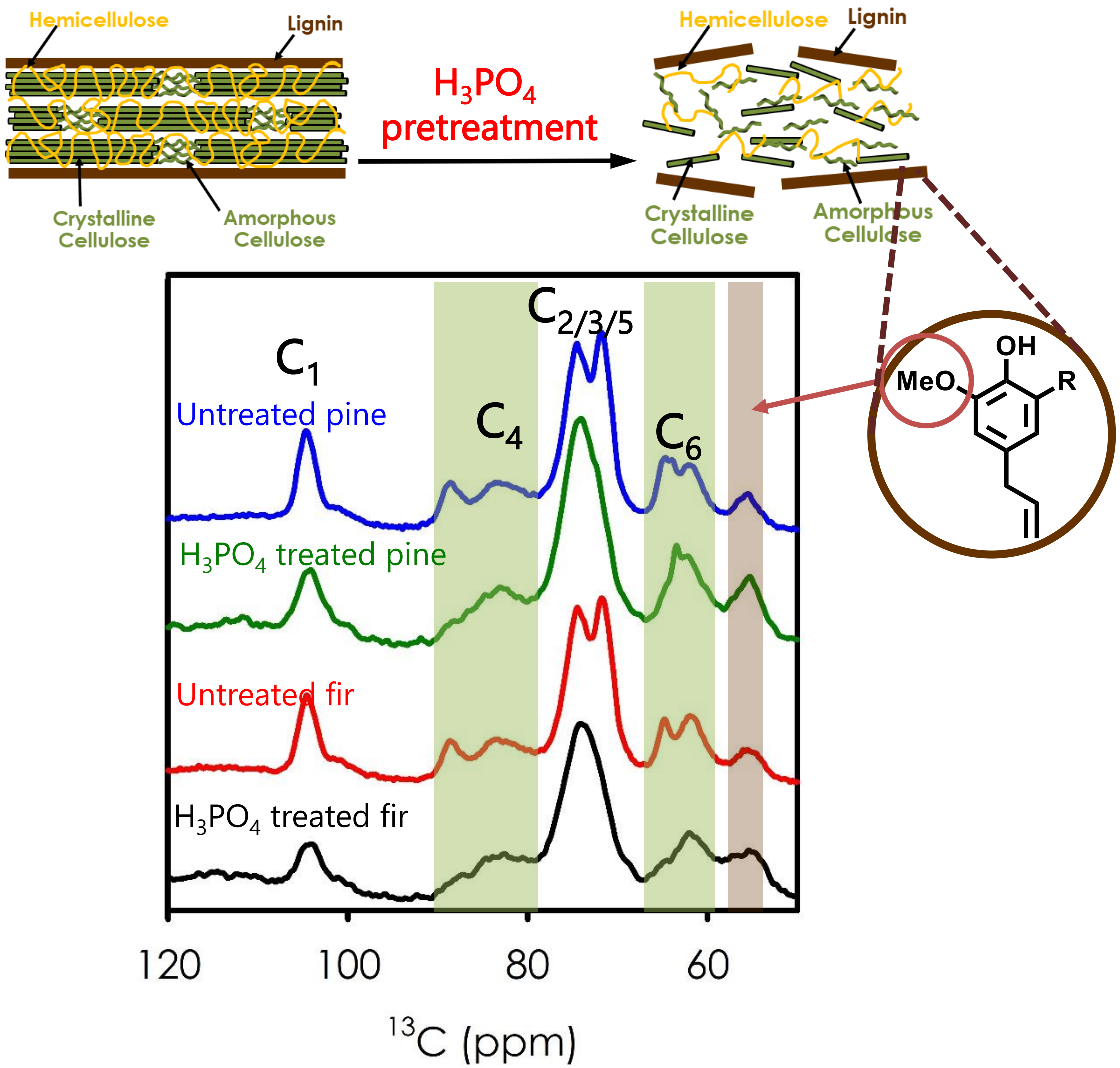

Figure 7. The crystallinity index of Avicel, untreated, and pretreated softwoods.

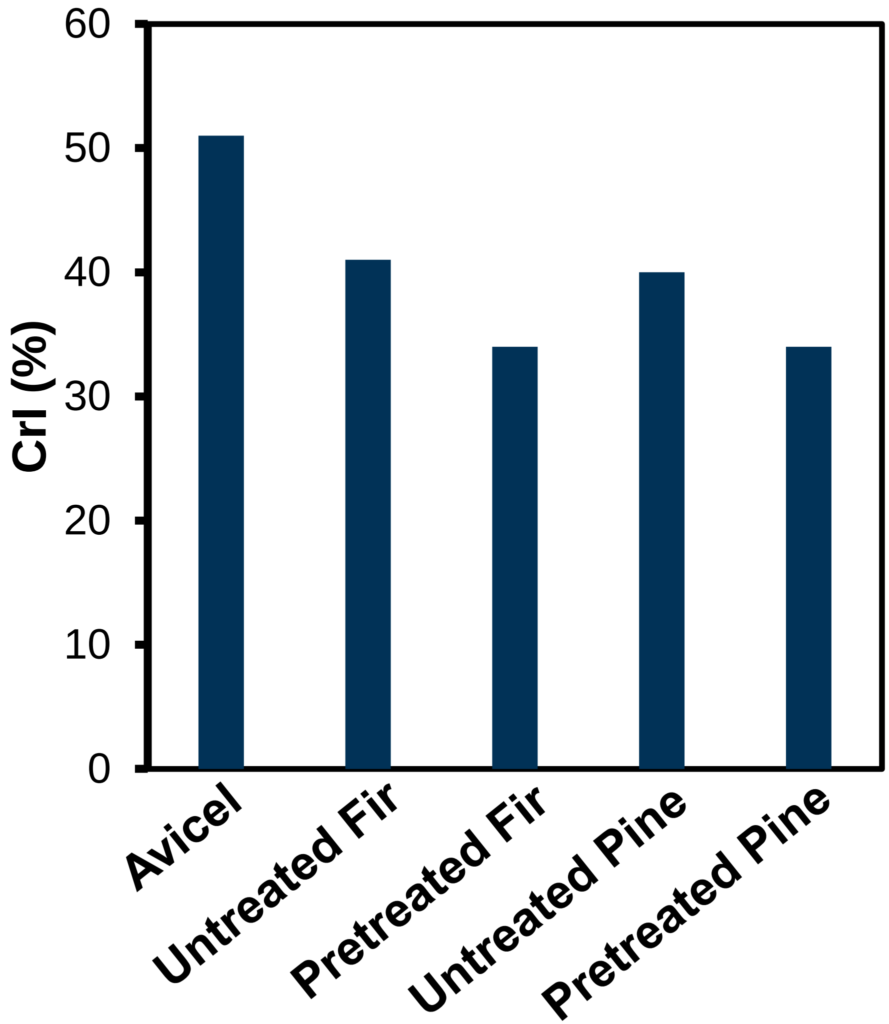

Figure 8. 2D ^{13}C-^{1}H HSQC NMR spectra in aliphatic region of Douglas fir and yellow pine before and after H_3PO_4 pretreatment.

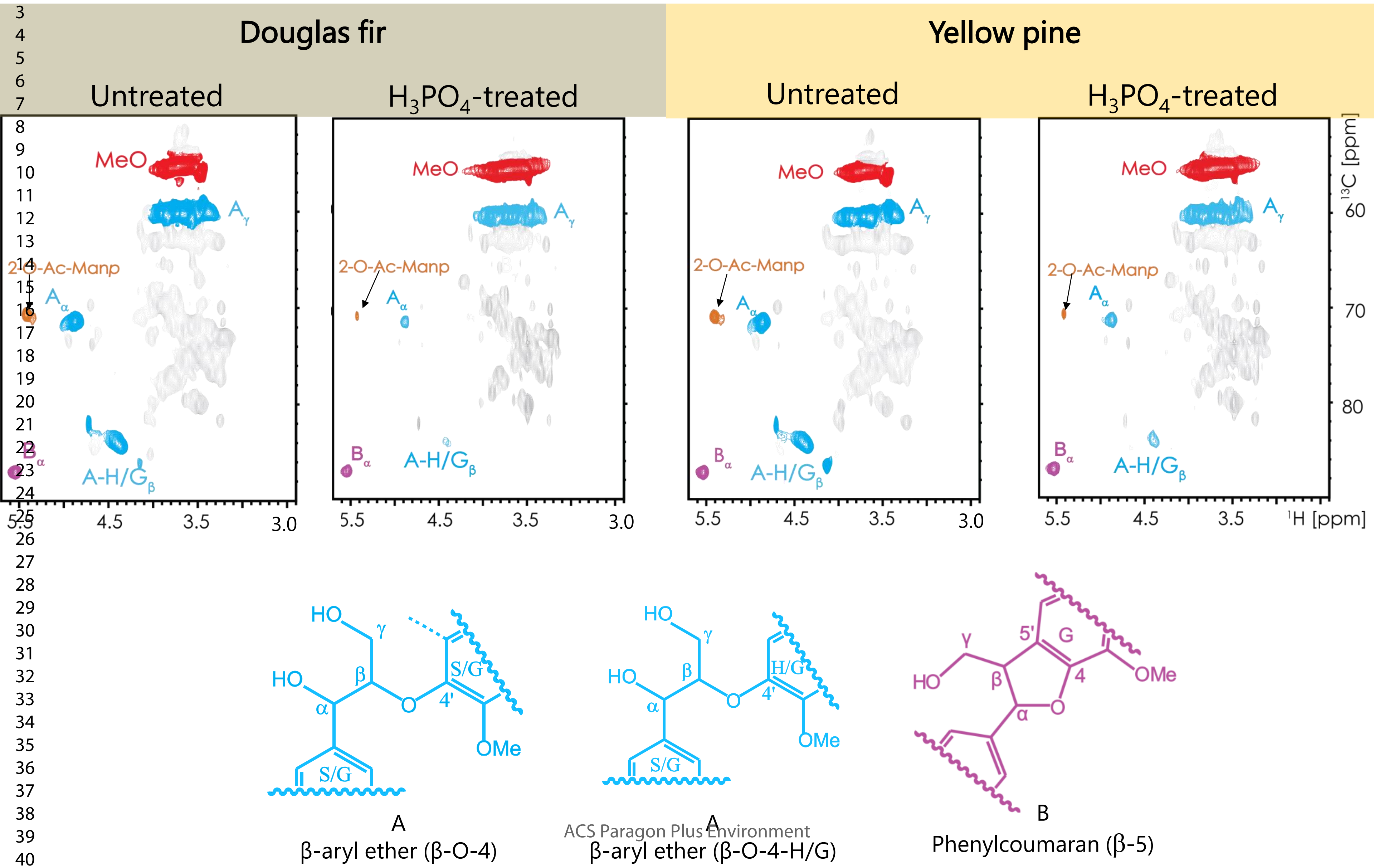

Figure 9. 2D ^{13}C-^{1}H HSQC NMR spectra in anomeric region of Douglas fir and yellow pine before and after H_3PO_4 pretreatment.

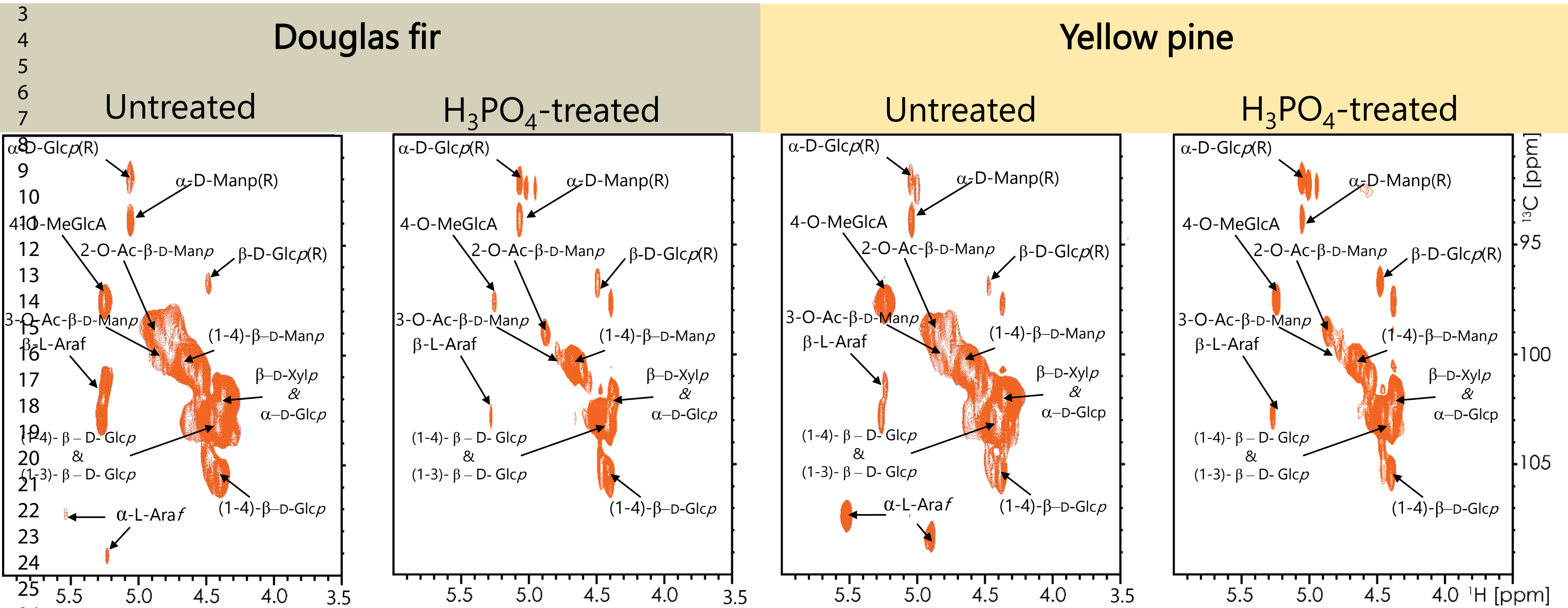

Figure 10. 2D ^{13}C-^{1}H HSQC NMR spectra in aromatic region of Douglas fir and yellow pine before and after H_3PO_4 pretreatment.

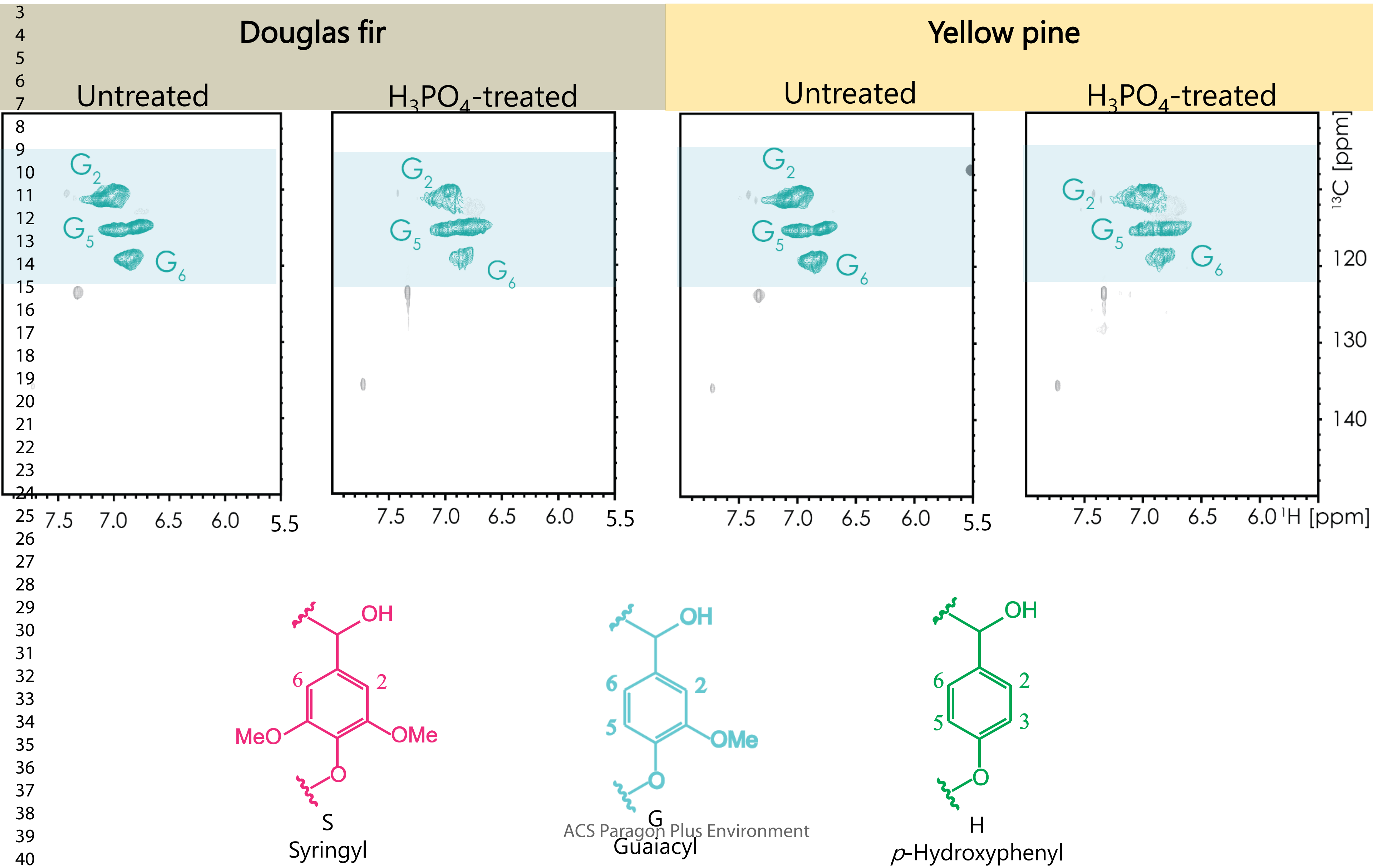

Figure 11. H_3PO_4 pretreatment accommodates all types of feedstocks; agricultural wastes, bioenergy crops, and woody biomass.

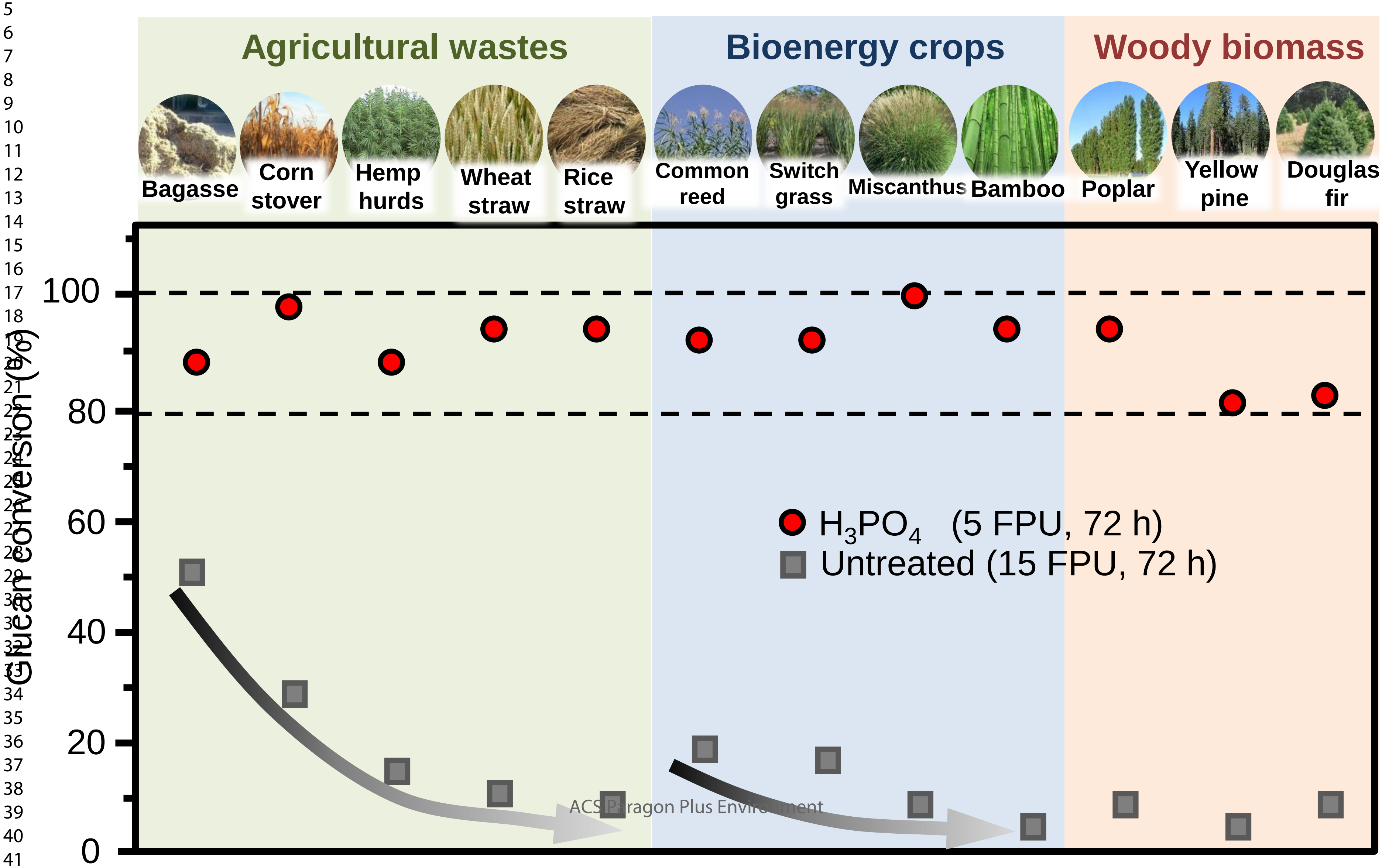

Graphical abstract